



**EFFECT OF HOT CHAMBER PARAMETER ON THE GAS FLOW  
IN THE THERMAL TRANSPIRATION PUMP**



**BACHELOR OF MECHANICAL ENGINEERING TECHNOLOGY  
(Technology Automotive) WITH HONOURS**

**2022**



**Faculty of Mechanical and Manufacturing Engineering  
Technology**



**EFFECT OF HOT CHAMBER PARAMETER ON THE GAS FLOW IN  
THE THERMAL TRANSPARATION PUMP**

**Ilman Hakim Bin Muhamad Jamaludin**

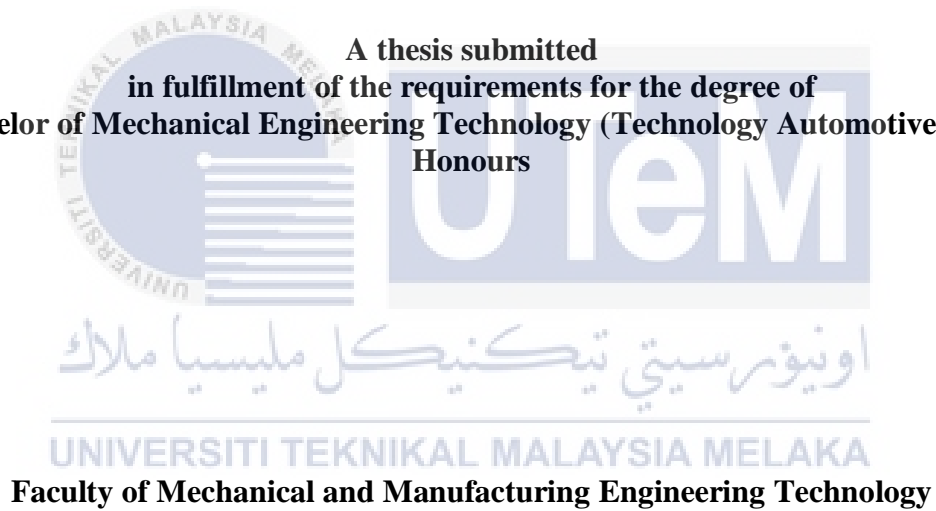
**Bachelor of Mechanical Engineering Technology (Technology Automotive) with  
Honours**

**2022**

**EFFECT OF HOT CHAMBER PARAMETER ON THE GAS FLOW IN THE  
THERMAL TRANSPIRATION PUMP**

**ILMAN HAKIM BIN MUHAMAD JAMALUDIN**

**A thesis submitted  
in fulfillment of the requirements for the degree of  
Bachelor of Mechanical Engineering Technology (Technology Automotive) with  
Honours**



**UNIVERSITI TEKNIKAL MALAYSIA MELAKA**

**2022**

## DECLARATION

I declare that this Choose an item. entitled “Effect of Hot Heat Exchanger Parameter on The Gas Flow in The Thermal Traspiration Pump” is the result of my own research except as cited in the references. The Choose an item. has not been accepted for any degree and is not concurrently submitted in candidature of any other degree.

Signature



Name

: Ilman Hakim Bin Muhamad Jamaludin

Date

: 11/1/2023

UNIVERSITI TEKNIKAL MALAYSIA MELAKA

## APPROVAL

I hereby declare that I have checked this thesis and in my opinion, this thesis is adequate in terms of scope and quality for the award of the Bachelor of Mechanical and Manufacturing Engineering Technology (BMMA) with Honours.

Signature : 

Supervisor Name : Sushella Edayu Binti Mat Kamal

Date : 20/1/2023



## DEDICATION

I would like to express my dedication from the bottom of my heart specially to my parents Muhamad Jamaludin Bin Yasin and Wan Pisah Binti Wan Jaafar for providing me moral as well as financial support throughout the years. Not to forget my siblings, friends, and my Final Year Project members for their unconditional support throughout the process. I would like to thank my supervisor madam Sushella Edayu Binti Mat Kamal for the full endless support and guidance for me to finish my Final Year Project. This project seems impossible without her guidance to keep me on the right track. Last but not least, all these bittersweet moments and memories upon completing my studies and research will always be cherish.

اونيورسيتي تيكنيكل مليسيا ملاك

UNIVERSITI TEKNIKAL MALAYSIA MELAKA

## ABSTRACT

The Knudsen pump (KP) is a type of micropump that may produce thermally induced flows in rarefied gas environments. These flows are caused by temperature fields in the environment. It offers the benefits of having no moving components, having a basic structure, being easy to construct and extend, having access to a wide variety of energy sources, and having a low overall energy usage. This project focuses on designing hot chamber with heating element. As the heating element being heated, it will produce hot gas within the chamber. Thus, the gas flow as well as the temperature difference can be analyzed. As the heating element is used to heat up the chamber, a thermocouple which functions as sensor that is used to measure the temperature as it is placed inside the hot chamber. After the temperature rises to desired value, the gas flow is then can be analyzed and observed. The observation is made by witnessing the hot gas flow transferred from the hot chamber to a narrow channel which then transferred to cold chamber. The comparison of temperature difference can be compared by the data observed.

## **ABSTRAK**

*Pam Knudsen (KP) ialah sejenis pam mikro yang mungkin menghasilkan aliran teraruh istilah dalam persekitaran gas jarang. Aliran ini disebabkan oleh medan suhu di persekitaran. Ia menawarkan faedah tanpa komponen yang bergerak, mempunyai struktur asas, mudah dibina dan dilanjutkan, mempunyai akses kepada pelbagai jenis sumber tenaga, dan mempunyai penggunaan tenaga keseluruhan yang rendah. Projek ini memberi tumpuan kepada mereka bentuk ruang panas dengan elemen pemanas. Apabila elemen pemanas dipanaskan, ia akan menghasilkan gas panas di dalam ruang. Oleh itu, aliran gas serta perbezaan suhu boleh dianalisis. Memandangkan elemen pemanas digunakan untuk memanaskan ruang, termokopel yang berfungsi sebagai sensor yang digunakan untuk mengukur suhu kerana ia diletakkan di dalam ruang panas. Selepas suhu meningkat kepada nilai yang dikehendaki, aliran gas kemudiannya boleh dianalisis dan diperhatikan. Pemerhatian dibuat dengan menyaksikan aliran gas panas dipindahkan dari ruang panas ke saluran sempit yang kemudiannya dipindahkan ke ruang sejuk. Perbandingan perbezaan suhu boleh dibandingkan dengan data yang diperhatikan.*





## ACKNOWLEDGEMENTS

In the Name of Allah, the Most Gracious, the Most Merciful

First and foremost, I would like to thank and praise Allah the Almighty, my Creator, my Sustainer, for everything I received since the beginning of my life. I would like to extend my appreciation to the Universiti Teknikal Malaysia Melaka (UTeM) for providing the research platform. Thank you also to the Malaysian Ministry of Higher Education (MOHE) for the financial assistance.

My utmost appreciation goes to my main supervisor, Sushella Edayu Binti Mat Kamal from Faculty Mechanical and Manufacturing, UTeM for all her support, advice and inspiration. Her constant patience for guiding and providing priceless insights will forever be remembered. Also, to my academic supervisor, Universiti Teknikal Malaysia Melaka (UTeM) who constantly supported my journey. My special thanks go to Amiera Husna student master at Universiti Teknikal Malaysia Melaka (UteM) for all the help and support I received from him.

Last but not least, from the bottom of my heart a gratitude to my beloved parents Muhamad Jamaludin Bin Yasin and Wan Pisah Binti Wan Jaafar, for their encouragements and who have been the pillar of strength in all my endeavors. My eternal love also to all my teammates for their patience and understanding. Finally, thank you to all the individuals who had provided me the assistance, support and inspiration to embark on my study.

## TABLE OF CONTENTS

	<b>PAGE</b>
<b>DECLARATION</b>	
<b>APPROVAL</b>	
<b>DEDICATION</b>	
<b>ABSTRACT</b>	<b>i</b>
<b>ABSTRAK</b>	<b>ii</b>
<b>ACKNOWLEDGEMENTS</b>	<b>iii</b>
<b>TABLE OF CONTENTS</b>	<b>iv</b>
<b>LIST OF TABLES</b>	<b>vii</b>
<b>LIST OF FIGURES</b>	<b>viii</b>
<b>LIST OF APPENDICES</b>	<b>x</b>
<b>CHAPTER 1 INTRODUCTION</b>	<b>11</b>
1.1 Background	11
1.2 Problem Statement	12
1.3 Research Objective	12
1.4 Scope of Research	13
<b>CHAPTER 2 LITERATURE REVIEW</b>	<b>14</b>
2.1 Introduction	14
2.2 Knudsen Pump	15
2.2.1 Thermal Transpiration pump	17
2.3 Vacuum Pump without a Moving Part and its Performance	18
2.4 Type of Heat Exchangers	22
2.4.1 Shell and Tube Heat Exchangers	22
2.4.2 Plate Heat Exchanger	23
2.5 Heat Exchanger Flow Configuration	24
2.5.1 Cocurrent Flow	25
2.5.2 Countercurrent Flow	26
2.5.3 Crossflow	26
2.5.4 Cross/counterflow	27
2.6 Types of Heating Elements	28
2.6.1 Transformer Type Heating Element	28
2.6.2 Molybdenum Disilicide Heating Element	30
2.6.3 Heating element coated with conductive polymer	32
2.6.4 Carbon Fibre Heating Element	32

2.6.5	Metal Characteristic Fiber Heating Element	33
2.6.6	Flexible Heating Element	33
2.7	Performance Test of Electric Heating Element	34
2.8	Thermal Insulation Cover	36
2.8.1	Mineral Wool	36
2.8.2	Investigation of thermal insulation performance of glass/carbon fiber-reinforced silica aerogel	37
2.8.3	Cellulose Aerogel	39
<b>CHAPTER 3 METHODOLOGY</b>		<b>41</b>
3.1	Introduction	41
3.2	Project Flowchart Process	42
3.3	Gantt Chart	43
3.4	Proposed Methodology	44
3.4.1	Experimental Set up	46
3.4.2	Configuration of Hot Chamber	48
3.5	Parameter Studies	51
3.5.1	Heating Element Design	51
3.5.2	Temperature Gradient	52
3.5.3	Type of Insulation	52
3.6	Limitation of Proposed Methodology	53
3.7	Summary	54
<b>CHAPTER 4 DISCUSSION</b>		<b>Error! Bookmark not defined.</b>
4.1	Effect of temperature at hot chamber	<b>Error! Bookmark not defined.</b>
4.2	Default testing without rockwool and wiremesh	56
4.2.1	Graph Temperature (°C) vs Time (minutes) without cooling system	57
4.2.2	Graph Temperature (°C) vs Time (minutes) with cooling system	58
4.2.3	Graph Time vs Temperature Ratio between Tc1 (without cooling system) and Tc2 (with cooling system)	59
4.3	Rockwool (with and without cooling system)	60
4.3.1	Graph Temperature (°C) vs Time (minutes) without cooling system	61
4.3.2	Graph Temperature (°C) vs Time (minutes) with cooling system	62
4.3.3	Graph Comparison Time vs Temperature ratio of rockwool between Tc1 (without cooling system) and Tc2 (with cooling system)	63
4.4	Rockwool + Wiremesh (with and without cooling system)	64
4.4.1	Graph Temperature (°C) vs Time (minutes) without cooling system	<b>Error! Bookmark not defined.</b>
4.4.2	Graph Temperature (°C) vs Time (minutes) with cooling system	<b>Error! Bookmark not defined.</b>
4.4.3	Graph Comparison Time vs Temperature Ratio of rockwool + wiremesh between Tc1 (without cooling system) and Tc2 (with cooling system)	65
4.5	Heat Distribution on Thermal Camera	68
<b>CHAPTER 5</b>		<b>Error! Bookmark not defined.</b>
5.1	Conclusion	72
5.2	Recommendation	73

5.3	Project Potential	73
	<b>REFERENCES</b>	<b>74</b>
	<b>APPENDIX</b>	<b>77</b>



## LIST OF TABLES

TABLE	TITLE	PAGE
Table 2-1	Heat Exchanger flow comparisons	28
Table 2-2	Composite properties with various ratios of glass fiber and carbon fiber (Ebert, HP, 2011).	38
Table 3-1	Gantt chart PSM 1	43
Table 5-4	Rockwool + wire mesh (with and cooling system)	80



## LIST OF FIGURES

FIGURE	TITLE	PAGE
Figure 2.1	Knudsen pump diagram (Retrieved from: <a href="https://www.semanticscholar.org/paper/Human-powered-Knudsen-pump-for-pneumatic-delivery.">https://www.semanticscholar.org/paper/Human-powered-Knudsen-pump-for-pneumatic-delivery.</a> )	15
Figure 2.2	Common Knudsen pump channel structures (Zhang, et. al, 2019).	17
Figure 2.3	Diagram of thermal transpiration pump path channel	18
Figure 3.1	Project flowchart planning	42
Figure 3.2	Stainless steel chamber	44
Figure 3.3	Inside view of stainless steel chamber	45
Figure 3.4	Inner chamber surface dimension	45
Figure 3.5	Inner hole dimension	46
Figure 3.6	Schematic diagram of thermal transpiration pump	47
Figure 3.7	Full system of thermal transpiration pump	48
Figure 3.8	Picolog Data Logger	49
Figure 3.9	PicoLog Interface	49
Figure 3.10	Thermostat	50
Figure 3.11	Power supply setup configuration	50
Figure 3.12	Heating element installation	51
Figure 3.13	Mineral wool insulation cover	53
Figure 4.1	Initial testing without rockwool and wire mesh	56
Figure 4.2	Graph Temperature versus Time without cooling system	57
Figure 4.3	Graph temperature versus time with cooling system	58

Figure 4.4 Graph time versus temperature ratio	59
Figure 4.5 Rockwool (with and without cooling system)	60
Figure 4.6 Graph temperature vs time (without cooling system)	61
Figure 4.7 Graph temperature versus time (with cooling system)	62
Figure 4.8 Graph comparison temperature ratio versus time	63
Figure 4.9 Hot chamber with wire mesh and covered by rockwool	64
Figure 4.10 Graph temperature versus time of rockwool and wire mesh without cooling system	65
Figure 4.11 Graph Temperature ( $^{\circ}\text{C}$ ) versus Time (minutes) with cooling system	66
Figure 4.12 Graph temperature ratio versus time	67
Figure 4.13 Heat distribution on thermal camera for empty hot chamber	70
Figure 4.14 Heat distribution on thermal camera for installed wire mesh chamber	71

## LIST OF APPENDICES

APPENDIX	TITLE	PAGE
APPENDIX 1	Gantt chart PSM 2	78
APPENDIX 2	Data default testing without rockwool and wire mesh	78
APPENDIX 3	Data rockwool (with and without cooling system)	79





# CHAPTER 1

## INTRODUCTION

### 1.1 Background

Mechanical gas pumps are distinguished from nonmechanical pumps, which are distinguished by the presence or absence of moving parts. Mechanical pumps drive fluid flow by utilizing the mechanical energy of its moving parts, and the working mediums of mechanical pumps are primarily liquids. Because of the moving parts, their life spans, sensitivity, and stability are all significantly reduced. On the contrary, fluid flow is driven by nonmechanical kinds of energy such as electric, thermal, chemical and magnetic energy in nonmechanical pump applications. In addition to liquids, they can work with gases and solids in the form of nanometer-sized particles as well as solids in the form of nanometer-sized particles.

Knudsen pumps functioning mechanism is based on thermal creep effect. Many academics have long been interested in KPs because of its advantages of having no moving parts, simple architectures, a wide variety of energy sources, low energy consumption, and the ease with which they can be mass produced and expanded.

## 1.2 Problem Statement

A Knudsen Pump (KP) is a form of thermal transpiration that may generate thermally induced flows as a result of temperature fields configuration of Knudsen pump which has hot temperature and cold temperature flow. This project will concentrate on designing a hot chamber using heating element which will be connected to alternating current electricity power supply. This will produce hot gas which roughly 100 °C to 150 °C inside the chamber as the heating element heated up the chamber. However, the chamber suffered significant heat loss due to conduction, which occurs when heat is transported to the chamber surface, causing the temperature to drop.

On the contrary, by creating a thermal insulation cover to enclose the chamber, it is possible to limit the amount of heat lost. This is due to the fact that insulating materials are poor conductors, and hence could help to prevent heat loss by conduction. It will also be the emphasis of this project to design the insulating chamber cover, which will be necessary in order to attain and maintain the desired temperature inside the chamber.

## 1.3 Research Objective

The main objectives of this project design are as follows:

- a) To review and identify the parameters that effect the performance of thermal transpiration pump.
- b) To evaluate the effect of hot chamber parameters on the temperature.
- c) To analyze the effect of temperature difference on the gas flow properties in the thermal transpiration pump.

## 1.4 Scope of Research

The scope of this research are as follows:

- Designing hot chamber with heating element for Knudsen pump thermally induced flow system
- Designing thermal insulator cover applicable for hot chamber
- Conduct a temperature analysis before and after the insulator cover has been installed.



## CHAPTER 2

### LITERATURE REVIEW

#### 2.1 Introduction

The thermally induced flow of rarefied gas is well understood to be caused by the temperature gradient along the walls of the Knudsen pump, and the gas is propelled to flow from the low-temperature side to the high-temperature side. That is the fundamental mechanism of the Knudsen pump, which was proposed in 1909 by Danish physicist Martin Knudsen. The Knudsen pump can deliver continuous gas flow and has no moving parts, a simple structure, ease of operation, a long-life span, low energy consumption, and a wide range of energy sources. The traditional rectangular Knudsen pump is made up of a succession of wide and narrow micro-channels that are alternately connected. By imposing high-temperature and low-temperature heat resources at the two ends of the large channels, a tangential temperature gradient arises. This causes the gas flow to experience thermal creep.

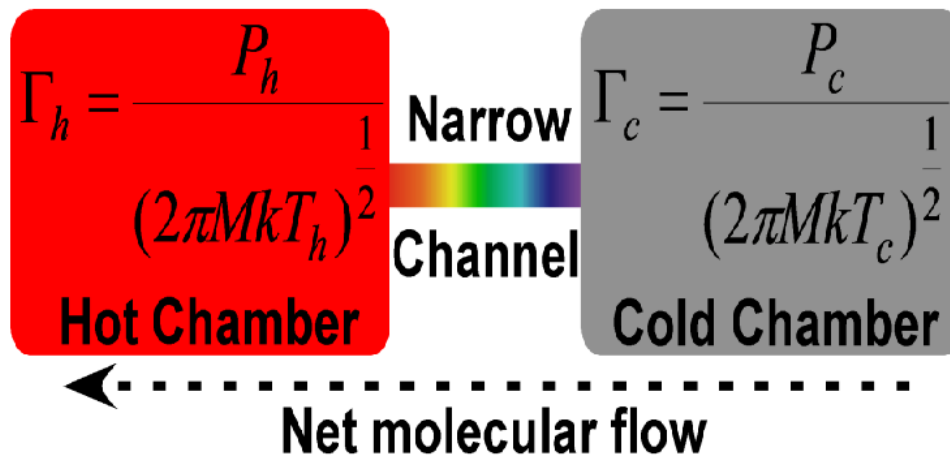


Figure 2.1 Knudsen pump diagram (Retrieved from:

<https://www.semanticscholar.org/paper/Human-powered-Knudsen-pump-for-pneumatic-delivery.>)

## 2.2 Knudsen Pump

(Zhijun Zhang, et. al, 2019) explained that the traditional rectangular Knudsen pump is made up of a number of large and narrow micro-channels that are connected to one another in alternating fashion. When high-temperature heat resources are introduced at one end of the wide channels and low-temperature heat resources are introduced at the other end, a tangential temperature gradient is produced. Because of this, a thermal creep effect is produced for the flow of the gas. In recent years, with the development of materials technology and micro-machining technology, it has become possible to produce the pump structure by using poly-silicon material. Additionally, the flowing channel of the Knudsen pump can now be constructed by using the inter-molecular gaps in porous materials such as aerogel membranes, mixed cellulose ester (MCE), zeolite, porous ceramics, and Bi<sub>2</sub>Te<sub>3</sub>.

Since the rectangular Knudsen pump has been suggested, numerous configurations for the channel have been constructed and investigated in succession. (Zhijun Zhang, et. al,

2019) added that there are a number of studies that use the DSMC approach to analyze the flow of gas mixtures. It has been discovered through the modelling of DSMC that the Knudsen pump demonstrates a good capability in gas separation. Studies on Knudsen pumps have, for the most part, concentrated on developing new aspects of the structure, developing methods to improve performance, and developing applications in the real world.

Most of the gas that is utilised in simulations is a monatomic noble gas. On the other hand, gas mixes have been used more frequently than individual gases, and the proportions of noble gases found in the atmosphere are extremely low. In addition, the width of the micro-channel has already reached the nanoscale level, which ensures that the Knudsen pump is able to function normally even when subjected to air pressure.

By imposing high-temperature and low-temperature heat resources at the two ends of the large channels, a tangential temperature gradient arises. This causes the gas flow to experience thermal creep. With the advancement of materials technology and micro-machining technology in recent years, the pump structure can now be produced by using poly-silicon material and the inter-molecular gaps in porous materials such as aerogel membranes, mixed cellulose ester (MCE), zeolite, porous ceramics, and  $\text{Bi}_2\text{Te}_3$ . Since the rectangular Knudsen pump was introduced, other channel structures have been built and examined. There are different types of Knudsen pump channel structures as shown in figure 2.2 which are curved-straight channel, double-curves channel, sinusoidal channel, matrix channel, ratchet channel, an taper channel.

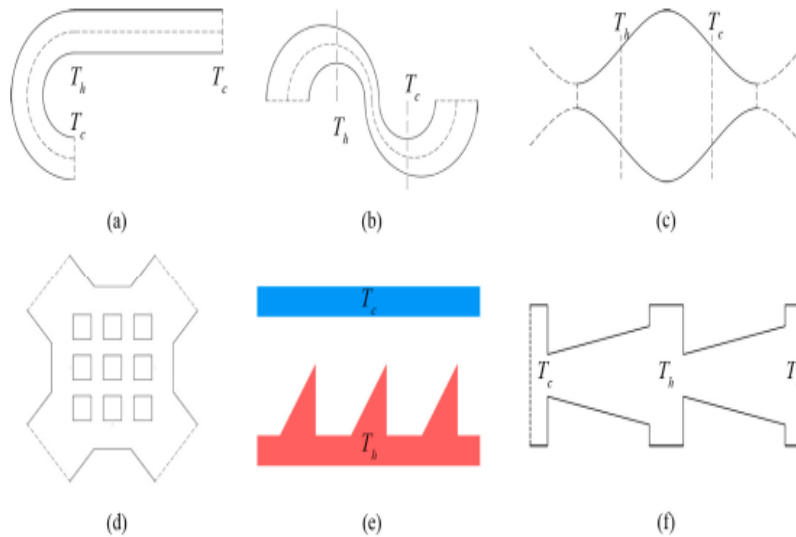


**Figure 2.2 Common Knudsen pump channel structures (Zhang, et. al, 2019).**

### 2.2.1 Thermal Transpiration pump

(Reynold's, et al, 1879) independently began their investigation into the process of heat transpiration which was the year they published their findings. Thermal transpiration is the movement of gas molecules from the cold side to the hot side of a channel that is being subjected to a temperature gradient. The flow of gas molecules is confined to either the free molecular or transitional gas flow regimes within the channel. In order for transpiration to be of any significance, the hydraulic diameter, denoted by  $d$ , must be less than the mean free path, denoted by  $k$ , of the gas molecules; in other words, the Knudsen number, denoted by  $Kn(k/d)$ , must be bigger than unity. In the example shown in Figure 1, which consists of two large chambers connected to one another by nanochannels and situated within a thermal transpiration element, the ratio of the equilibrium pressures is found by taking the square root of the difference in absolute temperature between the two chambers. (This is simply an estimate, but it is accurate for the case of free molecular flow under perfect conditions.) Knudsen was the first person to demonstrate that it would be possible to construct a system

for the stationary pumping of gas that was based on this phenomenon (Knudsen, 1909). However, because materials with suitably narrow channels were not readily available until the 21st century, the majority of the Knudsen pumps that were documented up until that time worked at pressures lower than the atmospheric pressure.

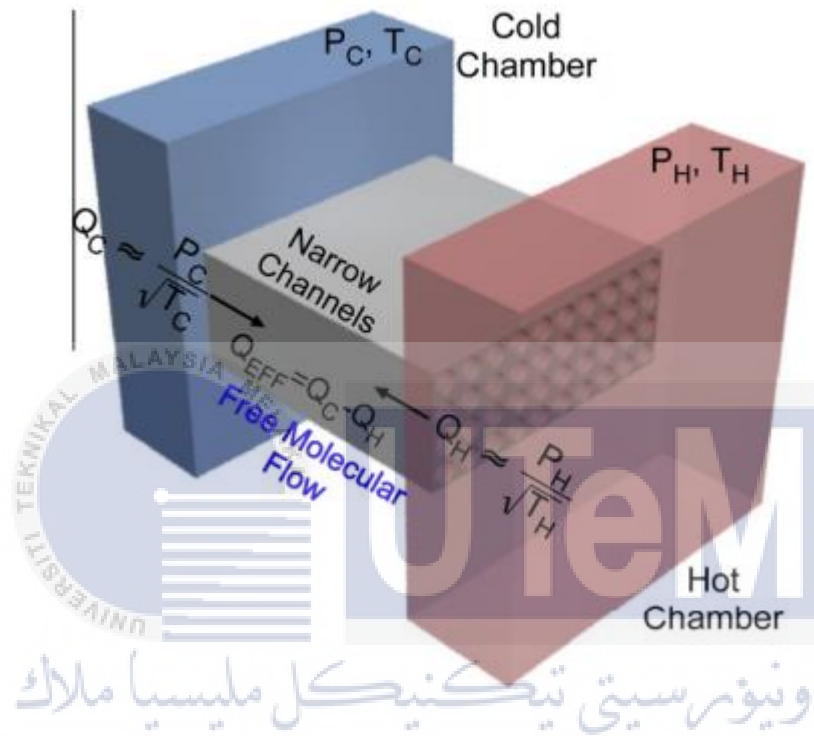


Figure 2.3 Diagram of thermal transpiration pump path channel

### 2.3 Vacuum Pump without a Moving Part and its Performance

According to (Sone, Yoshio, 2003), The presence of a temperature field can have a significant impact on the mobility of a rarefied gas. The thermal transpiration, which is an example of a flow that is induced by a pipe that has a temperature gradient along it, is a well-known example, and its application to a vacuum pump that does not have a moving part has been considered for a considerable amount of time. A pressure differential is produced when two reservoirs that are connected by a conduit that has a temperature gradient (or reservoirs of different temperatures) are brought together. due to the process of thermal transpiration,



various temperatures). To maintain a significant pressure difference between the two reservoirs, the temperature difference between them must be maintained at a significant level. This is not a workable solution, hence a cascade method needs to be developed instead. Knudsen conducted an experiment with a cascade system as early as 1910, and he successfully demonstrated the system's usefulness. A pumping system that makes use of the flow is gaining fresh attention. This is due to the fact that the system does not have any moving parts and does not involve any mixing process.

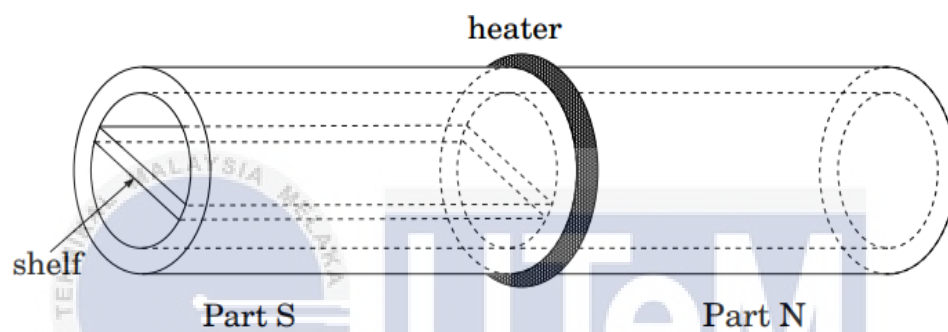


**Figure 2.4 A pipe with a shelf put up partition (Sone, Yoshio, 2003)**

From the figure above, we can see that the heater is placed outside of the chamber, the shelf is used as a partition. The flow in the pipe or channel is made to go in only one direction. One-way flows can be seen as a result of the corresponding experiment (or during one segment of the previously described pipe that has both of its ends maintained at the same temperature and pressure). For the induction of the one-way flows, the ditch is absolutely necessary. In point of fact, there is no evidence that a one-way flow can be created in a pipe or channel that is straight using numerical modelling, experimental research, or mathematics. Another system is presented that allows a one-way flow to be induced without the presence of average pressure and temperature gradients, and the flow is experimentally confirmed. As can be seen in figure above, it has the form of a circular pipe that is both straight and halved, with a shelf or shelves installed in the halved portion, and a heater located in the middle of

the pipe. When Knudsen numbers are small, the thermal transpiration (temperature-induced flow) via a pipe's cross sectional area is proportional to the mass flux through the pipe, but the Poiseuille flow through the pipe is proportional to the square of the cross sectional area (pressure-driven flow). This disparity in the mass fluxes provides a clear explanation for the unidirectional flow that occurs in the second system.

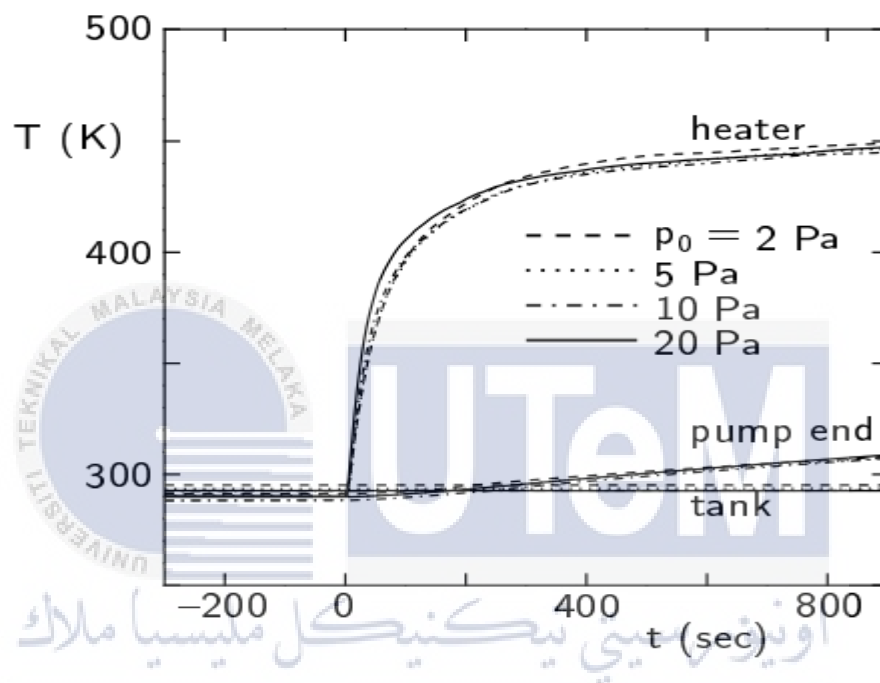


**Figure 2.5 Graph Temperature (K) vs Time (sec) (Sone, Yoshio, 2003).**

From the figure above we can see that the heating element started to heat up the chamber with maximum temperature of 450 kelvin with respective time of 800 seconds. From the figure we can also stated that along the length of the pipe that connects the pumping system to the tan, a temperature gradient is produced. This is because when using the same source of energy, the temperature produced by the heater will vary. It is anticipated that the temperature at the heater will be lower for higher pressure within the scope of the pressure range and the size of the pipe used in the experiments. The amount of heat that is allowed to escape increases as the pressure rises. The thermocouple that is supposed to measure the

temperature at the heater that is positioned among the thinner pipes does not appear to be completely linked to the heater or the pipes. The heat transfer from the heater or the pipes is what determines the temperature that is displayed by the thermocouple. A sizeable portion of this heat transfer occurs through the gas that is present in the area between the thermocouple and the heater or the pipes. This goes up when the pressure goes up, and the thermocouple displays a higher temperature for the higher pressure. This line of reasoning is backed up by several additional studies. The temperature that is displayed at the heater in the numbers is lower than the actual temperature, as these figures are merely an approximate measurement of the temperature.

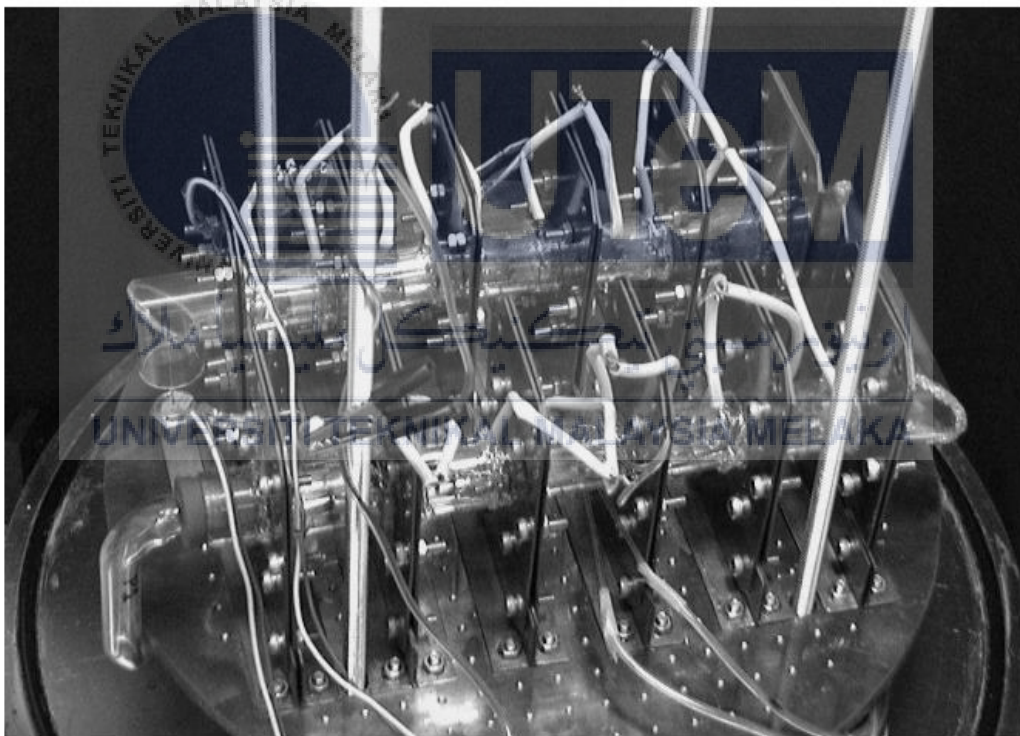


**Figure 2.6 Gas Pumping System (Sone, Yoshio, 2003).**

According to the experiment that have been conducted by (Sone, Yoshio, 2003). They setup the experiment using a round glass pipe with a heater in the centre and various channels on one side. That is, a bundle of 18 glass pipes of inner diameter 1.6 mm and length

15 mm is inserted in a half part of a circular glass pipe of inner diameter 15 mm and length 30 mm; a heater of Nichrome wire is wound around one end of each thinner pipe and placed in the central part of the 30 mm pipe; and a copper plate with thickness 1 mm is attached at each end of the unit. The thinner pipe side is S and the other N. The copper plate is both the junction to the next unit and the support, which is fixed to the base of a thick copper plate and keeps the pipe unit ends at a constant temperature similar to room temperature. The unit uses cross section variation and passage division. One induces one-way flow, whereas the other induces pressure differential. The bundle of thinner pipes divides the channel, and the cross section changes at the S-N division. The pump system has ten units. Due to the size of our bell jar for its performance trial, two subsystems consisting of five units coupled with copper plates in a series are connected. Glass pipes connect the subsystems.

## **2.4 Type of Heat Exchangers**

### **2.4.1 Shell and Tube Heat Exchangers**

According to (Ahmad Hajatzadeh et al, 2019). Shell tube heat exchangers are a type of heat exchanger that is utilised in a variety of chemical industries, including oil refineries. This exchanger is made out of a big cylindrical reservoir (shell) under high pressure and a bundle of tubes inside it, as the name implies. The fluid travels through the tubes and the heated stream flows on the tubes and within the shell.

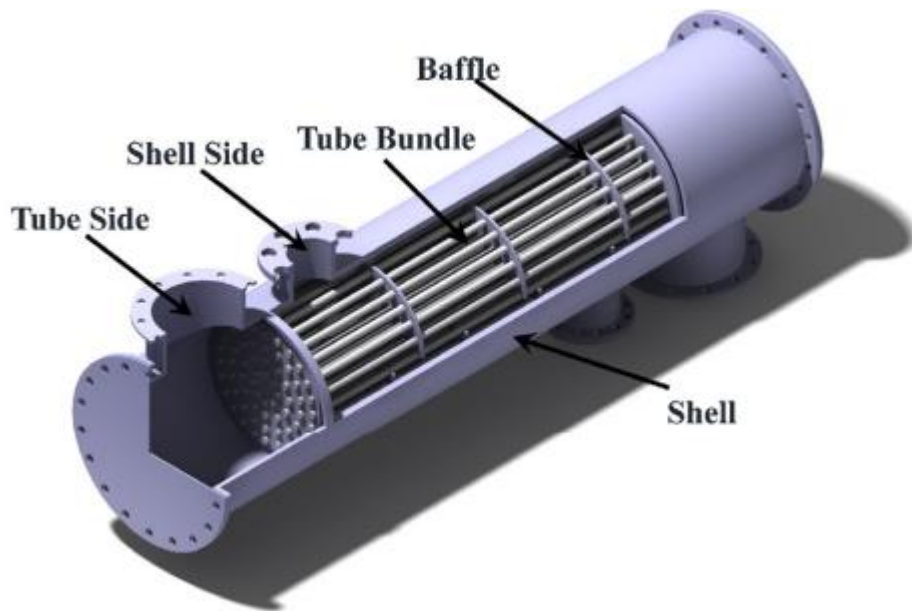


**Figure 2.7 Labelled Diagram of Shell Tube Heat Exchanger, (Ahmad Hajatzadeh Pordanjani, et al, 2019).**

#### **2.4.2 Plate Heat Exchanger**

According to (Ji Zhang, et al, 2019), plate heat exchangers are the most advanced type of heat exchangers available in the modern era and find widespread application across a variety of business sectors. This type of heat exchanger is preferred over double-walled resources and coil resources for the production of domestic hot water because it is simpler to repair, keep clean, and maintain than those other types of heat exchangers. Its application has expanded from the food industry to include the automotive industry, petrochemical industry, pharmaceutical industry, papermaking industry, building glass industry, air conditioning industry, oil and gas industry, and other industries. The use of a nanofluid working fluid, which is a suspension of solid nanoparticles in conventional heat transfer fluids, is one of the newest methods that has been developed in order to increase the thermal efficiency of plate heat exchangers and equipment. This method is also one of the most

innovative methods. The enhancement provided by these sorts of exchangers is improved when these fluids are used. However, utilising these novel fluids in heat exchangers is connected to a number of issues, one of which is a drop in pressure.

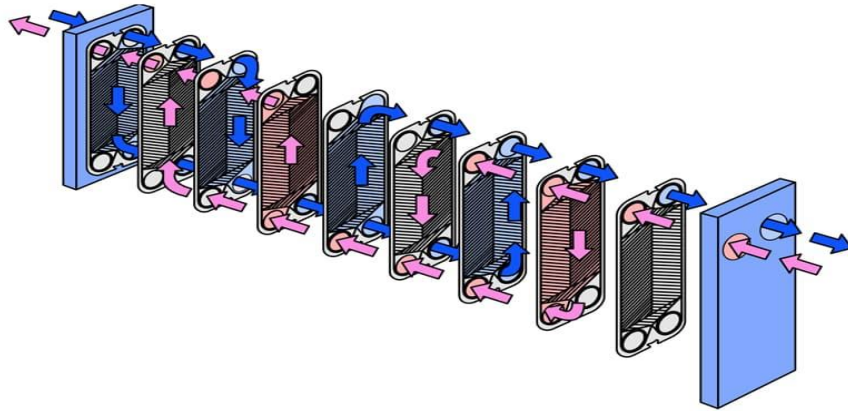


**Figure 2.8 Plate Heat Exchanger** (Retrieved from: <https://www.micetcraft.com/guide-to-plate-heat-exchangers/>).

## 2.5 Heat Exchanger Flow Configuration

This term relates to the direction of movement of fluids within a heat exchanger with respect to one another, and it is also known as the flow configuration or the flow arrangement in some cases. Heat exchangers can be configured in one of four different ways, according to their flow characteristics. The first flow configuration is known as concurrent flow. In cocurrent flow heat exchangers (sometimes referred to as parallel flow heat exchangers), the fluids move parallel to and in the same direction as each other, resulting for efficient heat transfer. It is clear that this layout generally results in poorer efficiency than a counter flow arrangement, but it is also the configuration that allows for the greatest thermal homogeneity throughout the heat exchanger's wall surfaces.

Furthermore, in crossflow heat exchangers, fluids flow perpendicular to one another rather than parallel to one another. The efficiency of heat exchangers that use this flow arrangement are in the middle of the range of that of countercurrent and cocurrent heat exchangers, respectively.

### 2.5.1 Cocurrent Flow

This term relates to the direction of movement of fluids within a heat exchanger with respect to one another, and it is also known as the flow configuration or the flow arrangement in some cases. Heat exchangers can be configured in one of four different ways, according to their flow characteristics. The first flow configuration is known as concurrent flow. In cocurrent flow heat exchangers (sometimes referred to as parallel flow heat exchangers), the fluids move parallel to and in the same direction as each other, resulting for efficient heat transfer. It is clear that this layout generally results in poorer efficiency than a counter flow arrangement, but it is also the configuration that allows for the greatest thermal homogeneity throughout the heat exchanger's wall surfaces.

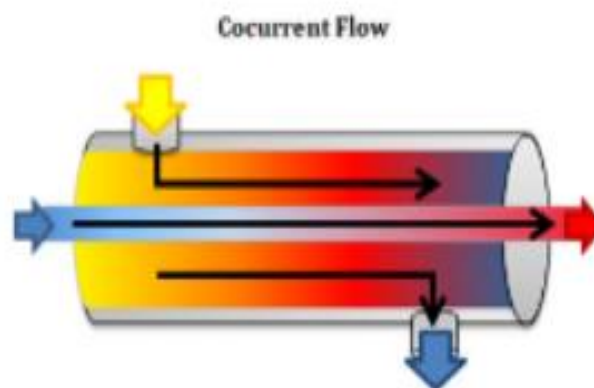


**Figure 2.9 Schematic diagram of cocurrent flow heat exchanger (Retrieved from: Thomas Publishing Company).**

## 2.5.2 Countercurrent Flow

On the other hand, countercurrent flow heat exchangers, sometimes referred to as counter flow heat exchangers, are heat exchangers in which the fluids flow in opposing directions to each other within the heat exchanger. They are also known as countercurrent flow heat exchangers and counter flow heat exchangers. Counter flow designs are the most often used of the flow configurations, and they typically display the highest efficiency because they allow for the greatest amount of heat transfer between fluids and, as a result, the biggest change in temperature.

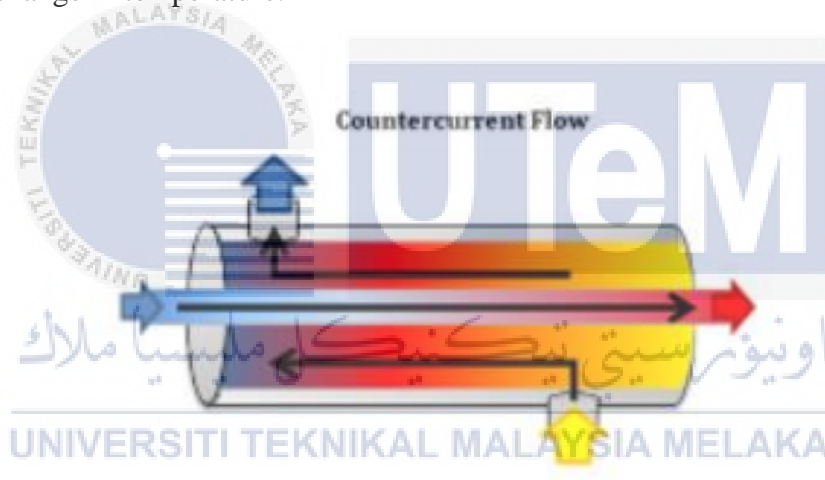


**Figure 2.10 Schematic diagram of countercurrent flow heat exchanger (Retrieved from: Thomas Publishing Company).**

## 2.5.3 Crossflow

Furthermore, in crossflow heat exchangers, fluids flow perpendicular to one another rather than parallel to one another. The efficiency of heat exchangers that use this flow arrangement are in the middle of the range of that of countercurrent and cocurrent heat exchangers, respectively.



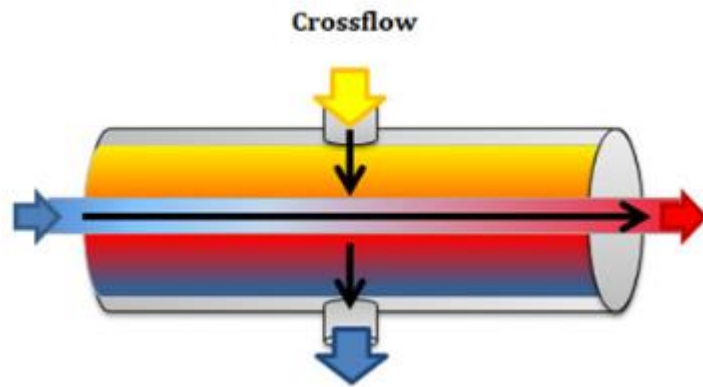


**Figure 2.11 Schematic diagram of crossflow heat exchanger (Retrieved from: Thomas Publishing Company).**

#### 2.5.4 Cross/counterflow

On top of that, Hybrid flow heat exchangers have features that are a blend of the characteristics of the flow arrangements previously discussed. Example: Within a single heat exchanger, designers can incorporate numerous flow passages and configurations (e.g., both counterflow and crossflow configurations) into the design. Space, budget, and temperature and pressure requirements are only a few examples of the constraints that these sorts of heat exchangers must overcome in a given application.

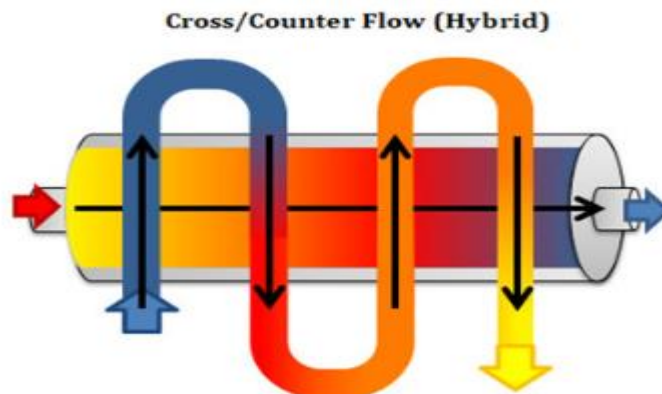


**Figure 2.12 Schematic diagram of cross/counter flow heat exchanger (Retrieved from: Thomas Publishing Company).**

**Table 2-1 Heat Exchanger flow comparisons**

No	Advantages	Diasadvantages
Cocurrent Flow	High flow rate	Hard to fix spaces due to large size
Countercurrent Flow	More resistant to scale formation	Can develop metal corossion
Crossflow	Compact design	High pressure loss
Cross/Counter Flow	More uniform rate of heat transfer	Lower capacity or volume

## 2.6 Types of Heating Elements

### 2.6.1 Transformer Type Heating Element

(Zar Ni N'ain, et. Al, 2017) states that in the steady-state mode of operation, which assumes that heat is transferred by natural convection, the heating element will experience its greatest temperatures. The environmental parameters were determined by using the thermophysical characteristics of water at a temperature of 85 degrees Celsius. (Serikov, et. Al, 2012) said that the electric heating element is a step-down transformer with a single-turn closedcoil secondary winding. This secondary winding acts as both a load and an element of the heating system. (Zar Ni N'ain, et. Al, 2017) added that this device makes it possible for

the whole heat-supply system to be more reliable, last longer, and be safer. This is due to the advantages that have been stated which is high electrical safety class, which is ensured by the multilayer electric insulation of the primary winding and the lack of an electric coupling between the secondary winding and the electrical network, as well as low coil voltage (less than 2 V) and a long effective life, since the structure provides an extended heat exchange surface with a heated environment, which slows down the process of scale formation and ensures thermal-state stability. Additionally, the durability is dependent on the appropriate selection of insulation materials, electromagnetic, loads, and dimension ratios. These are factors that significantly influence the temperature of the insulation and, as a consequence, the service life of the insulation and heating element as a whole. When compared to water heaters of the resistive type, heating elements of the transformer type have the primary drawback of having big dimensions and a substantial amount of weight. However, it is important to keep in mind that the weight and dimensions of the heating element do not typically account for the majority of the weight and dimensions of an entire electric water heating device consisting of a tank and a fluid to be heated consequently, these drawbacks are not typically a deciding factor in most situations. On the other hand, the structure of the heating element is made up of a three-phased spatial magnetic system 1 (shown in Figure 1), which is comprised of three rings 2 that have a tape made of cold-rolled electrical steel with variable width coiled around them.

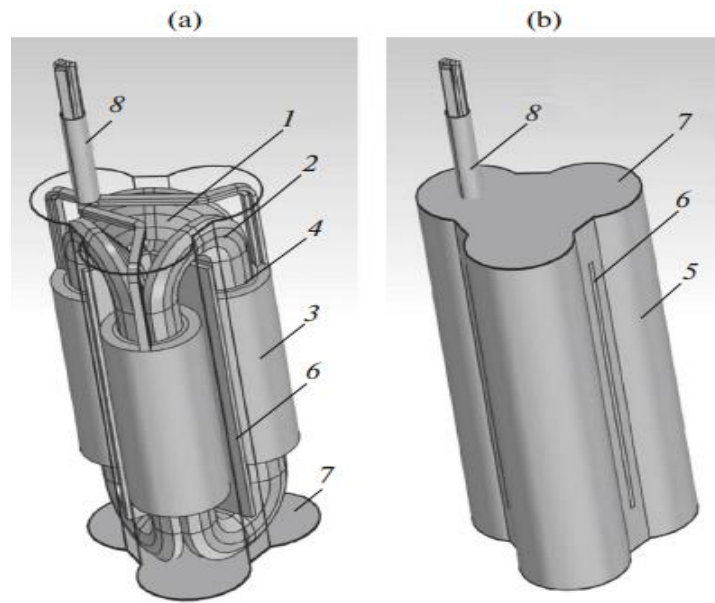


**Figure 2.13 Heating element of transfer type**

## 2.6.2 Molybdenum Disilicide Heating Element

(Shigetomo MATSUO et. Al, 1963) stated that all of the elements that belong to the Wa, Xa, and ya groups of the periodic table produce silicides that are electrically conductive, have a high melting point, and have a high oxidising resistance. A novel type of heating element has been created thanks to the utilisation of  $\text{MoSi}_2$ , which is distinguished among these silicides by having the highest oxidising resistivity. It has a temperature tolerance of up to 1,700 degrees Fahrenheit in air.

After being extruded into rods, powdered  $\text{MoSi}_2$  with polyvinyle-alcohol serving as a binder was subjected to a sintering process at a temperature of 1,600 degrees Celsius in the presence of hydrogen. Because the diameter of the heating element was made smaller at its main part and wider at its terminal sections where it was connected with a current-supply conductor, the heat was mostly created in the part of the heating element that was located at

its main part. A building of this kind was made possible by first fabricating the major (heat-generating) elements and the terminal parts independently, and then joining them together at 1900.

At the heating part of the rod, the flexural strength was measured at 30 kg/mm<sup>2</sup>, although it was significantly higher at the terminal parts. Electrical resistance was found to be  $3 \times 10^{-5}$  cm at ambient temperature and  $5 \times 10^{-4}$  cm when heated to 1,700 degrees Celsius. In open air, the surface density of electric power required to maintain a surface temperature of 1,700 degrees Fahrenheit was 60 W/cm<sup>2</sup>, but in an enclosed space, this value dropped to below one third. At a temperature of 1,000°C, the expansion coefficient was  $8.10^{-6}$ . Because the coefficient fluctuated approximately linearly with temperature but had a point of inflexion at around 250 degrees Fahrenheit, the process of cooling it must be carried out slowly in order to be effective. It exhibited flexibility at a temperature of roughly 1,800 degrees Fahrenheit, at which point it could be bent into any shape. This type of heating element can be utilised in any environment, including those containing oxidising and reducing gases, nitrogen, or vacuum.

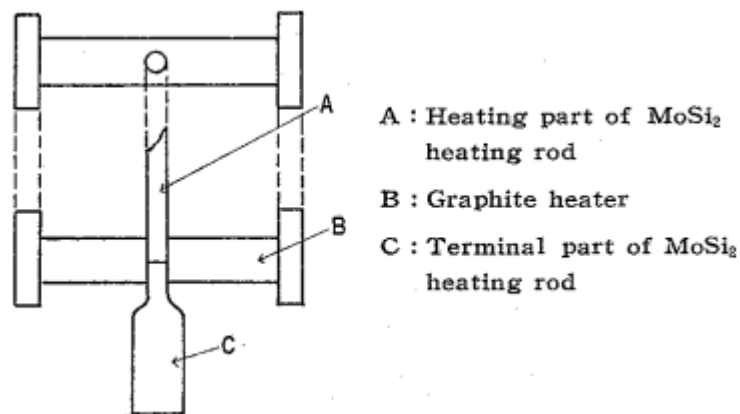


**Figure 2.14 Schematic explanation of the partial heating method for binding heating part and terminal**

### 2.6.3 Heating element coated with conductive polymer

(Gao, S., et al, 2020), claimed that conductive polymer is not only able to conduct electricity like metal, but it also has the properties of polymer. It is easy to make, has good conductivity that can be changed, has stable mechanical properties, is cheap, and is light. However, polymers have a long history of being recognised as insulating materials, and they are frequently utilised in the insulating of electrical cables and other electronic devices. However, there is also a variety of polymers that can conduct electricity in their own right. The presence of conjugated double bonds along the polymer backbone is the primary factor responsible for the electrical conductivity of these polymers.

### 2.6.4 Carbon Fibre Heating Element

From the article, according to (Gao, S., et al, 2020) there are two distinct varieties of heating elements made of carbon fibre: linear elements and surface elements. In order to take advantage of carbon fiber's exceptionally high tensile strength and good durability, the surface of the material used to produce hair wire has a layer of insulating protective coating applied to it. A linear heater can take on a variety of forms, each of which is determined by the requirements of a specific application. The surface heater is two-dimensional and may be electrically heated by embedding carbon fibres into conductive coating, carbon fibre paper, felt, film, sheet, and fabric. This creates a surface that is able to be electrically heated. On the other hand, in contrast to the linear heater, the surface heater does not have the capability of three-dimensional cutting adaptability, which is necessary for the production of garments.

### 2.6.5 Metal Characteristic Fiber Heating Element

According to (Gao, S., et al, 2020), pure metal fibre and metal-coated fibre are the two main types of metal-characteristic fibre. The former has great mechanical properties, such as high strength and modulus, good conductivity, high heat resistance, and high chemical stability. Now, cutting, drawing, and melt drawing are the ways to get ready. The last step is to coat the surface with metal. Some non-metallic matrix fibres can be made to conduct electricity by using certain methods. At the moment, you can plate metal in a number of ways, including with chemicals, electrolyte solutions, magnetron sputtering, immersion coating, etc.

### 2.6.6 Flexible Heating Element

According to (Shu Fang, et al. 2020), fabric lets air through and is easy to work into clothing, so putting conductive material into fabric is an important part of making flexible heating elements. Flexible heating fabrics can be made with metal wire, metal coating, metal nanowires, conductive polymer coating, carbon fibre, carbon nanotubes, graphene, and other conductive materials.

Fabric is heated by metal. Metal yarns. (Frank Hewitt, 1926) came up with a way to make heating fabric and heating pads as early as 1929 by putting wires into the fabric or pad to heat them with electricity. (Kayacan and Yazgan Bulgun, 2009) wove stainless steel yarns used as heating yarns into polyester knitting fabric. By putting one layer on top of another, the conductivity of each layer was compared. Figure 1 is made up of four layers of conductive fabric. In December 2019, the Web of Science will list the number of publications

with the key words "electric heating garment" and "electric heating element," sorted by year. The power density could be changed by changing the number of layers of conductive fabric, the number of conductive yarns, and the voltage that was applied. (Hamdani, 2015) stated knitted fabrics with heating wires made of elastic yarn, 316L stainless steel yarn, and braided silver-plated yarn on both sides of the heating wires. At a voltage of 3V, the highest equilibrium temperature of plain knitted fabrics was 84C, and the highest equilibrium temperature of interlock knitted fabrics was 99C. (Hao et al. 2012) stated woven silver filament or silver-plated yarns into the plain woven fabric at regular intervals. The design organisation chart could be used to change how long and thick the silver filament was. The heating fabric's resistance and power density could be changed to meet the needs. The study found that there is a strong positive linear correlation between the rated power and the maximum equilibrium temperature. This can help design and predict the physical properties of flexible heating fabric.

## 2.7 Performance Test of Electric Heating Element

According to (Gao, S. Et al, 2020), the change in resistance as temperature increases is known as thermal stability. In order to accurately measure the temperature of the fabric's surface, an infrared thermometer is required. A multimeter is required in order to accurately measure the fabric's resistance. Here is the formula of resistance change rate:

$$\lambda = \frac{R_0 - R_r}{R_r} 100\%$$

where  $\lambda$  represents the rate at which the resistance changes,  $R_0$  represents the initial resistance of the heating element, and  $R_r$  represents the resistance after the element has been heated. Temperature and time both influence the pace of heating. Using an infrared thermal



imager, one can determine the temperature by measuring the temperature of the core, which is located at the geometric centre of the cloth (with an interval of 10 seconds). The power density of an electric heating system is an indicator of its effectiveness. Here is the formula:

$$W = \frac{P}{S}$$

where W represents the power density, S [cm<sup>2</sup>] – the spraying area of composite fabric, while P represents the electric power according to (HAO, Y., et. al, 2019). According to (Song, W. F., et. al, 2015), the amount of heating will change how comfortable the fabric is, and too much heat in one spot can cause burns. Heating uniformity is the difference in the instantaneous temperature of each part of the heating fabric's surface, which can be described by the temperature distribution coefficient. The more even the distribution is, the smaller the coefficient.

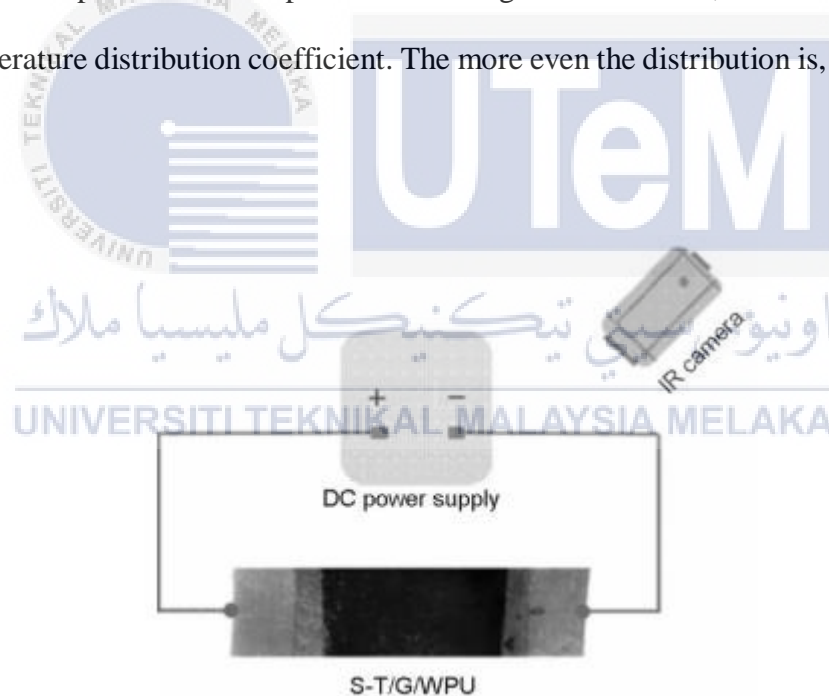


**Figure 2.15 Schematic diagram of electric heating performance test, (Gao, S., et al, 2020).**

## 2.8 Thermal Insulation Cover

### 2.8.1 Mineral Wool

(Bala'zs Nagy, et. Al, 2019) stated that a guarded hot plate apparatus was used in order to determine the heat conductivity of the mineral wool samples. The thermal conductivity of a building material can be evaluated using any one of a wide variety of accessible analytical approaches. These samples of stone wool were inhomogeneous, as was described previously, they are composed of a layer that is more difficult and a layer that is easier to work with. As a consequence of this, a speedy measurement of the thermal conductivity using procedures such as transient plane or line source methods would not supply a result that is accurate and precise. We decided to use the guarded hot plate method because the Taurus TLP 300 DTX apparatus provides the capability to measure up to 120 mm thickness using the guarded hot plate method. This enables us to determine the thermal conductivity and thermal resistance of various materials, including insulation and building components. The Taurus instrument is able to measure the thermal conductivity of the composite sample in the range of 0.01–0.5 W m<sup>-1</sup> K<sup>-1</sup> when the specimen is composed of vertical layers. This is accomplished by measuring the temperature difference on the hot and cold sides of the sample as well as the flow of heat through the layers. The measuring area is 50 mm 9 50 mm in the centre of the sample; however, the sample size needs to be in the range of 100 mm 9 100 mm to 300 mm 9 300 mm in order to provide undisturbed one-dimensional steady-state heat flow in the measured section. The sample size needs to be in the range of 100 mm 9 100 mm to 300 mm 9 300 mm in order to provide accurate results. If a sample is smaller than the maximum size, then additional edge protection to the sides of the sample is required in order to obtain an accurate measurement. In addition, the apparatus

features an isolated test chamber that eliminates the possibility of extraneous thermal impacts and air-cooled Peltier temperature plates that produce a sample mean temperature that falls somewhere in the range of 0 to 60 degrees Celsius. The electrical lifting device, digital pressure measurement, and sample thickness measuring are all included in the fenced-in hot plate that has safety features.



**Figure 2.16 Mineral wool, (Bala'zs Nagy, et. Al, 2019).**

### **2.8.2 Investigation of thermal insulation performance of glass/carbon fiber-reinforced silica aerogel**

According to (Ebert, HP, 2011), generally heat transfer in aerogel compounds depends on three things which are low heat conduction through the solid backbone, low heat transfer rate within the gaseous phase of the highly porous aerogel structure, and radiative heat transfer through photons. So, composite heat transfer has a lot to do with density (or the ratio of solid mass to volume, which shows how conduction works), porosity, and pore size, which show how free gas transfer works. Aerogel composites can be built using 10–20 percent carding CF as the heat insulation layer and GF layers for strengthening. Table 2.1 shows that when carding CF 5% was sandwiched between two GF layers, the composite's strength rose with heat conductivity from 0.031 to 0.0513 W/m K. CF content enhanced flexural strength and heat conductivity when GF was 5%. Heat conductivity increased from

0.032 to 0.042 W/m K, demonstrating that CFs affect composite strength and heat transfer.

Radiation may make CFs less cost-effective and heat-absorbing.

**Table 2-2 Composite properties with various ratios of glass fiber and carbon fiber**

(Ebert, HP, 2011).

Fiber Content (%)	Maximim Stress (MPa)	Thermal Conductivity (W/m.K)	Density (g/cm <sup>3</sup> )
GF3.5 + CF5	1.988	0.0335	0.138
GF5 + CF5	2.846	0.031	0.133
GF10 + CF5	2.909	0.0513	0.149
GF5 + CF3.5	2.174	0.042	0.144
GF5 + CF10	2.909	0.0322	0.135
GF5 + CF15	2.342	0.032	0.135

Carbon fibre insulation is widely recognized as one of the most environmentally friendly types of insulation available. Cellulose is a fibrous material that is made from recycled cardboard, paper, and other similar materials. It is used in the construction industry. It is available in a non-tight package. Coir has an R-value that varies between R-3.1 and 3.7, depending on the type of cellulose used in the production. Following the results of recent study on cellulose, some researchers believe that the material could be a fantastic ingredient to use in the prevention of fire damage. Carbon dioxide is virtually completely absent from the composition of cellulose due to the material's compactness. A fire can do significant damage since there is no oxygen available in the substance. As a result, the amount of damage caused by a fire is significantly reduced.

The fire resistance and environmental friendliness of cellulose make it one of the most environmentally friendly and environmentally useful types of insulation available today. While employing this material has several advantages, there are also downsides, such as the likelihood of allergic reactions to newspaper dust in some individuals. More to the point, when compared to other types of insulation, such as fibreglass, it is more difficult to obtain individuals who are knowledgeable about the installation and maintenance of this type of insulation. Despite this, cellulose is a low-cost and extremely effective insulator that can be used in a variety of applications.



**Figure 2.17 Cellulose Insulation (Retrieved from: attainable home, 2022).**

### **2.8.3 Cellulose Aerogel**

Regarding the influence that morphology has on the thermal performance of aerogels, (Sakai et. Al, 2016) examined the relationship between crystalline cellulose nanofibers in cellulose foams and aerogels with solid volume fractions ranging from 0.3 percent to 2.7 percent. The aerogels were made of cellulose foams. In the case of the foam, the thermal conductivity dropped as the solid volume portion became a larger percentage of the total volume. The conductivity of air within a microscale pore is, in principle, due to

convection, and hence, it has the same conductivity as the conductivity of air in the atmosphere. However, the non-interconnected layout of the porous structure allows for significant heat transfer between the air and the solid phase, which plays a significant influence in the total conductivity of the material. Because of this, the correlation between thermal conductivity and solid volume fraction can be seen as being caused by an increase in the contribution of the interfacial heat transfer, which occurs because the pore size decreases with an increase in solid volume fraction. When it came to aerogels, the thermal conductivity of the material improved as the proportion of solid volume increased. Because of the presence of open pores, there is almost no heat transmission between the solid phase and the gas phase in this scenario. Jiménez-Saelices et al. [20] also investigated the effect that the varied pore organisations had on the thermal characteristics of cellulose aerogels. Freeze-drying was used to transform cellulose nanofibril suspensions into aerogels. Two distinct moulds, each of which was treated to a distinct temperature gradient, were used in this process.

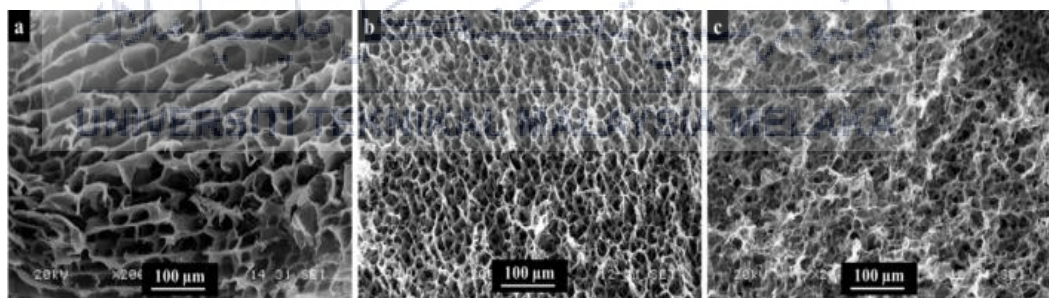


**Figure 2.18 SEM images of aerogel**

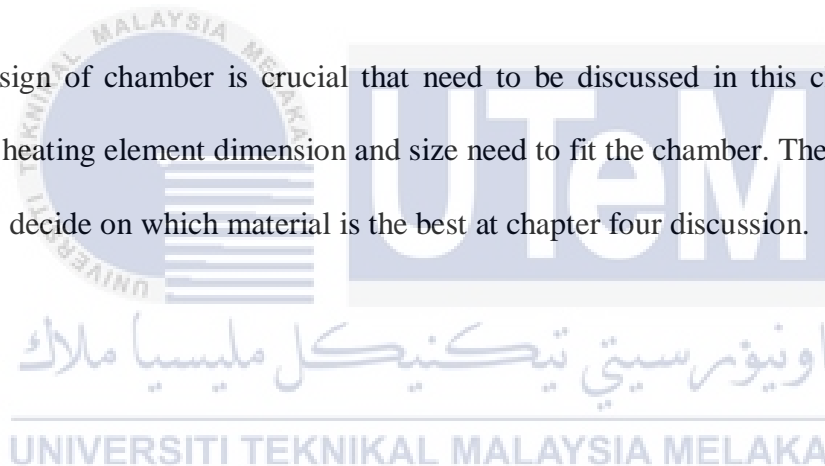
## CHAPTER 3

### METHODOLOGY

#### 3.1 Introduction

This thesis will specifically focus on designing hot chamber with heating element to analyze the gas flow in thermal transpiration pump. The detail step on how to design the hot chamber with heating element to analyze the gas flow will be discussed in this chapter.

Design of chamber is crucial that need to be discussed in this chapter. This is because the heating element dimension and size need to fit the chamber. The results will be discussed to decide on which material is the best at chapter four discussion.



### 3.2 Project Flowchart Process

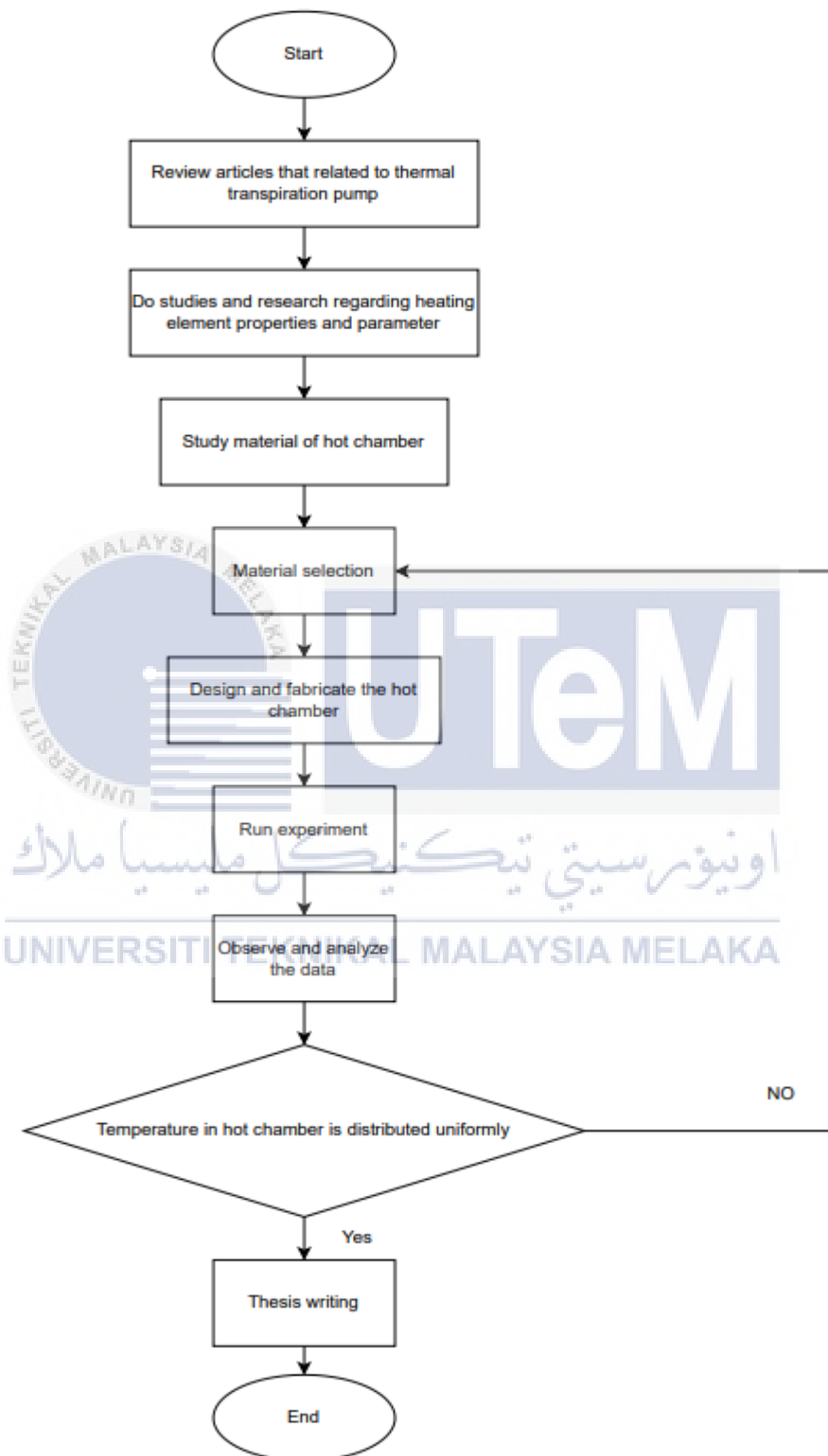


Figure 3.1 Project flowchart planning



### 3.3 Gantt Chart

Table 3-1 Gantt chart PSM 1

PSM1															
No.	Activity	WEEK													
		1	2	3	4	5	6	7	8	9	10	11	12	13	14
1	Problem statement	■	■												
2	Literature Review			■	■	■									
3	Material Selection <ul style="list-style-type: none"> <li>• Observation</li> <li>• Product detail comparison</li> </ul>			■	■	■	■	■	■						
4	Conceptual design							■	■	■					
5	Design selections										■	■			
6	Preparation & presentation												■	■	

### 3.4 Proposed Methodology

Hot chamber design is very crucial, this is because there are many aspects to look for and to be considered. The first thing to consider is how heat could be accumulated without much loss inside the chamber. Moreover, the chamber size and dimension must be figured out in order to place the heating element. The material of chamber is playing a huge role, this is because stainless steel could withstand high temperatures without failure due to high pressure.



**Figure 3.2 Stainless steel chamber**

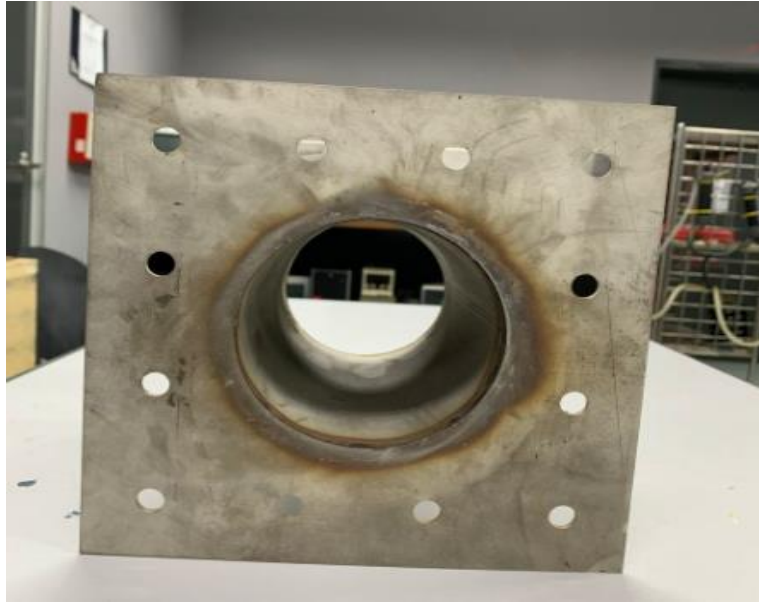


**Figure 3.3 Inside view of stainless steel chamber**

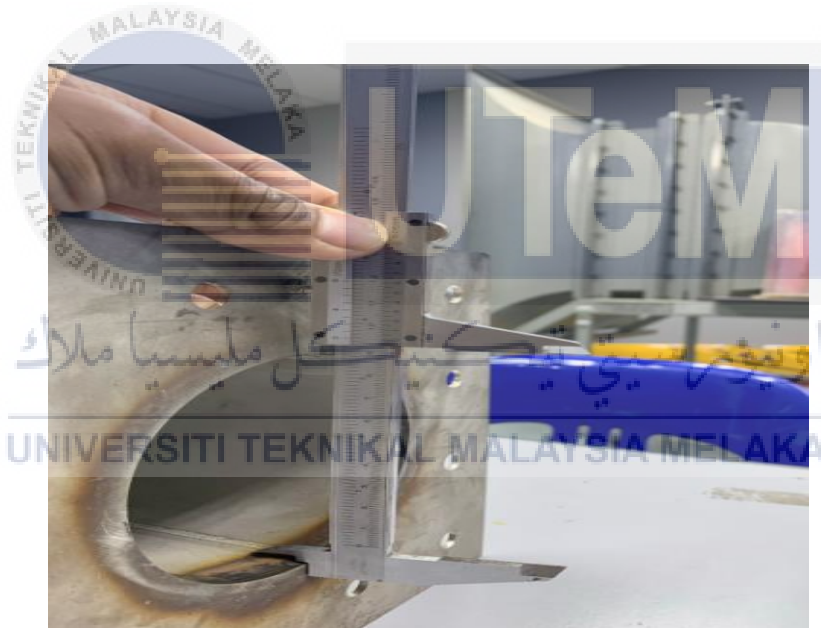


**Figure 3.4 Inner chamber surface dimension**



**Figure 3.5 Inner hole dimension**

### **3.4.1 Experimental Set up**

In thermal transpiration pump system, there are three important parts which are hot chamber, cold chamber, and porous media channel. This mechanism will induce gas flow without the use of mechanical parts to drive the gas from the hot end to the cold end of a narrow channel. In this system, the heating element will be heated until it produces hot gas with a high temperature. After the chamber temperature rises, the hot gas will flow to the cold end (cold chamber), which will cause the temperature to drop. Figure 3.6 below offers a straightforward interpretation of the complex idea of thermal transpiration. The rate of gas flow from one chamber to another is directly proportional to the pressure in that chamber and inversely proportional to the square root of temperature of that chamber. Suppose there are two chambers at different temperatures ( $T_H$ ,  $T_C$ ) that are connected by a short channel. As a result, there is an actual movement of gas molecules from the cold chamber to the hot chamber if the initial pressures in the two chambers are the same.

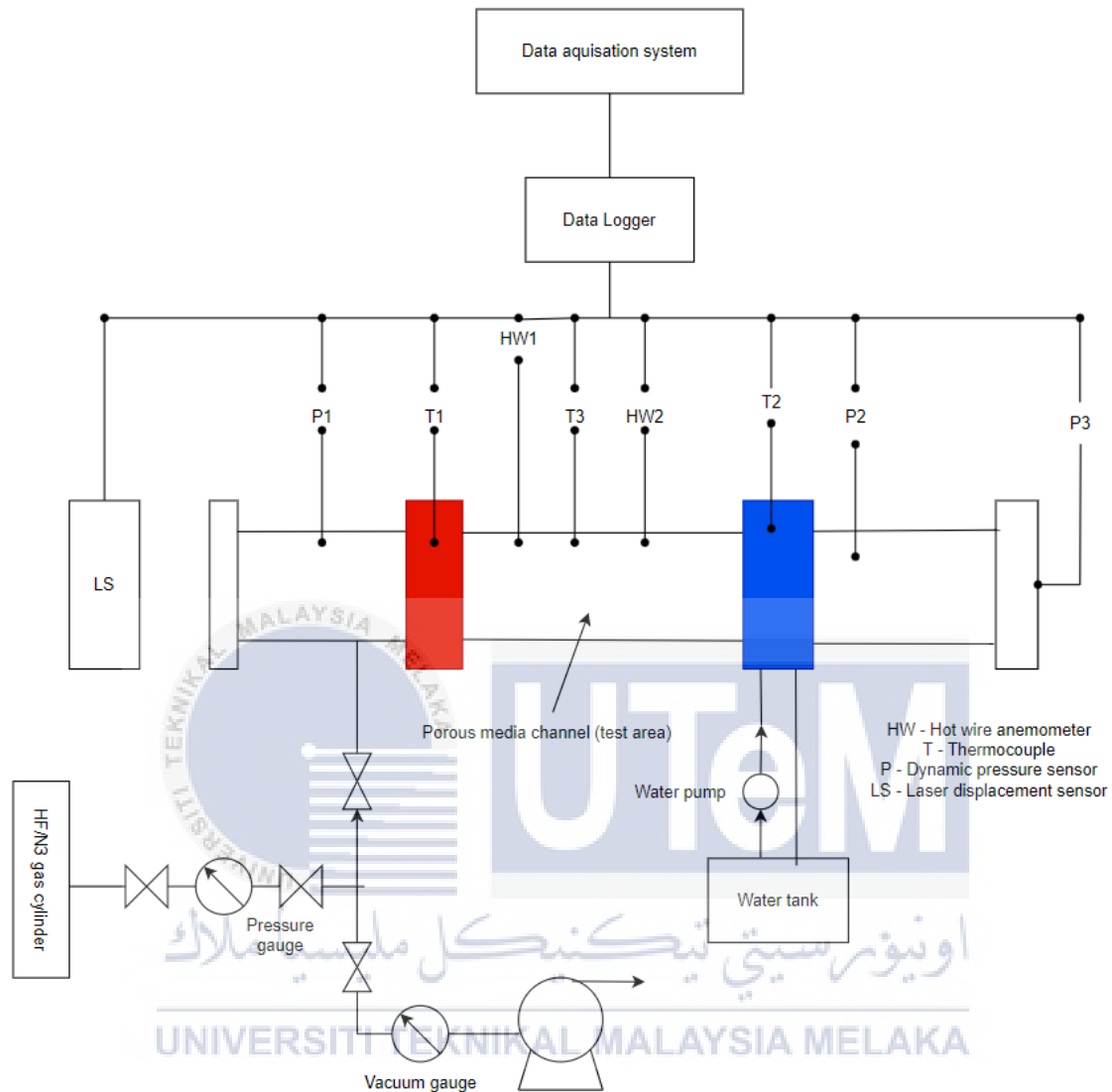


**Figure 3.6 Schematic diagram of thermal transpiration pump**

### 3.4.1.1 Full System of Thermal Transpiration Pump

In this particular setup, the hot chamber is located on the right-hand side of the figure 3.7, while the cold chamber is located on the left-hand side. The porous medium is located in the middle of the hot chamber and the cold chamber.

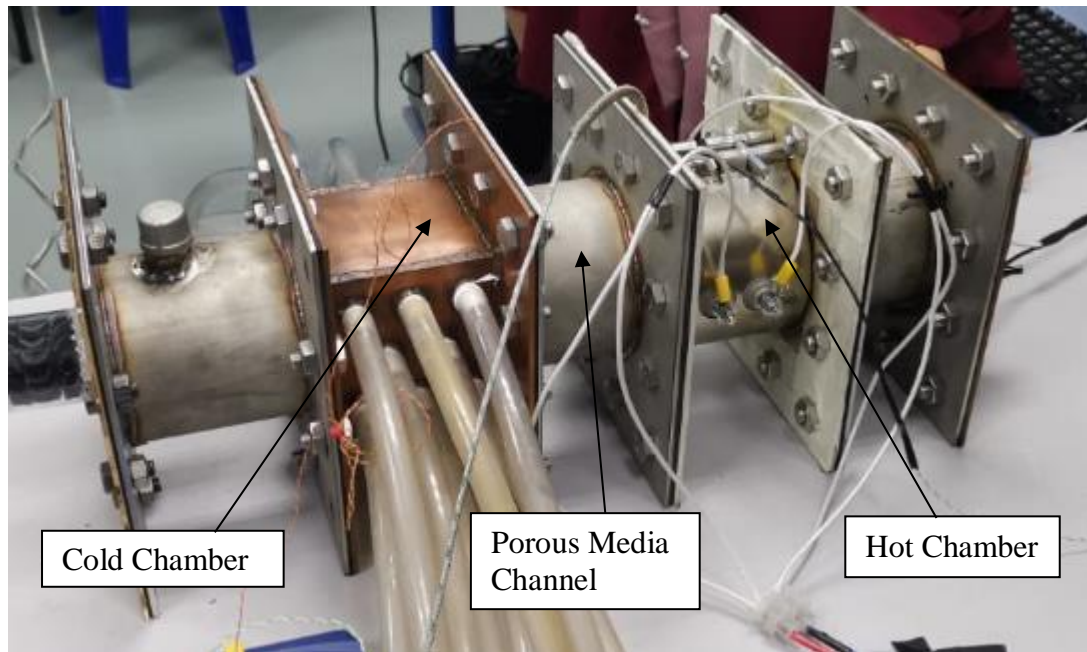


**Figure 3.7 Full system of thermal transpiration pump**

### **3.4.2 Configuration of Hot Chamber**

Hot chamber design is very crucial, this is because there are many aspects to look for and to be considered. The first thing to consider is how heat could be accumulated without much loss inside the chamber. Moreover, the chamber size and dimension must be figured out in order to place the heating element. The material of chamber is playing a huge role, this is because stainless steel could withstand high temperatures without failure due to high pressure.



**Figure 3.8 PicoLog Data Logger**

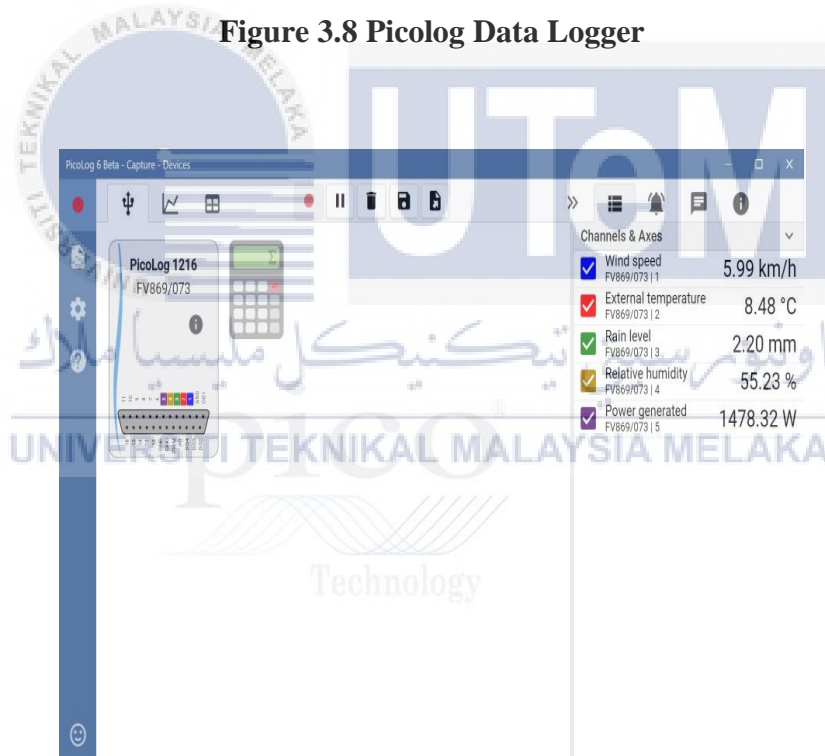


**Figure 3.9 PicoLog Interface**



**Figure 3.10 Thermostat**



**Figure 3.11 Power supply setup configuration**



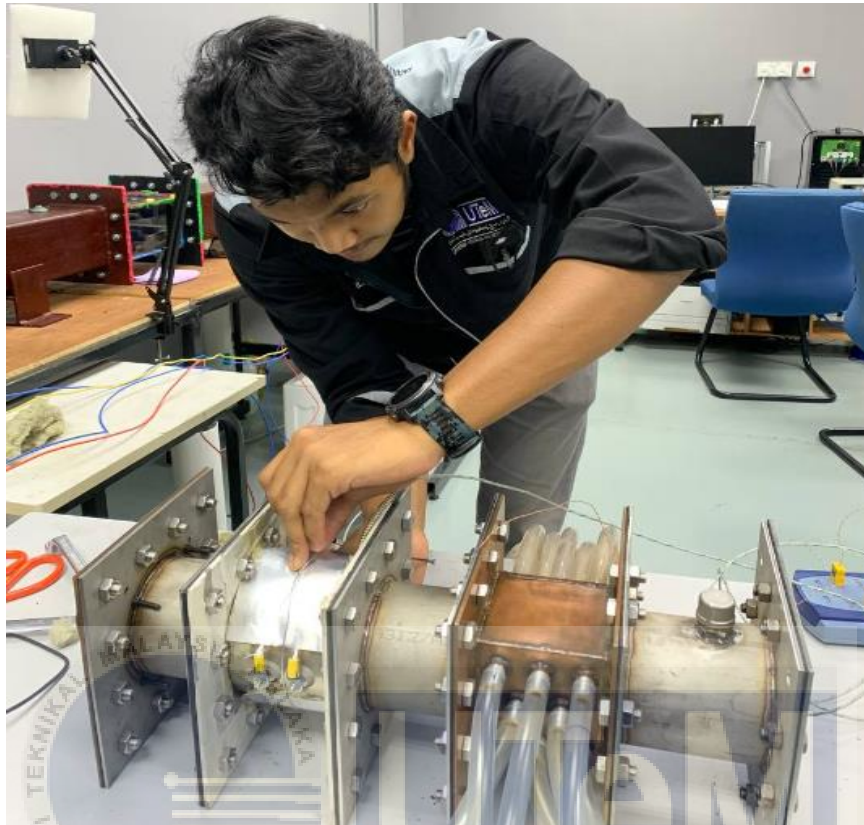


**Figure 3.12 Heating element installation**

### **3.5 Parameter Studies**

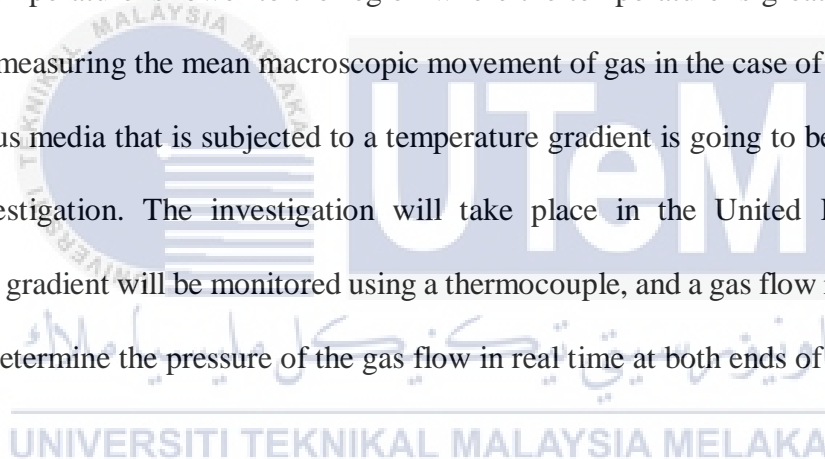
#### **3.5.1 Heating Element Design**

As a result of the design of the heating element that has been created, cross-sectional copper wire has been selected as the heating element. As a direct consequence of this decision, the temperature that was achieved was only sixty degrees, which was insufficient for the gas to flow. On the other side, when the temperature reached its maximum, the copper wire melted. As a result, the appropriate heating element, such as a ceramic heater, is required to guarantee that there is sufficient power to achieve the desired temperature.

Thermocouple is a piece of equipment that has been used to measure the temperature difference. Additionally, the use of this equipment is required in order to measure the temperature differences between the various materials that make up heating components.

### **3.5.2 Temperature Gradient**

Thermal transpiration is the movement of molecules of rarefied gas on a macroscopic scale that is driven by a temperature gradient. This movement is driven by a temperature difference. A temperature gradient will be produced when there is a difference in the temperatures of the hot chamber and the cold chamber. The gas moves from the region where the temperature is lower to the region where the temperature is greater. An original method for measuring the mean macroscopic movement of gas in the case of an acrylic tube with a porous media that is subjected to a temperature gradient is going to be put to the test in this investigation. The investigation will take place in the United Kingdom. The temperature gradient will be monitored using a thermocouple, and a gas flow rate sensor will be used to determine the pressure of the gas flow in real time at both ends of the capillary.



### **3.5.3 Type of Insulation**

Insulation made of rock wool has been chosen for this design because of the rock wool's favorable physical qualities, which allow it to withstand high temperatures. Heat is lost from the hot chamber as it is being prepared for installation, and the temperature falls very quickly over the course of this preparation. This is because the open chamber allows for a significant amount of heat to escape. As soon as it is put in place, the temperature of

the hot chamber will remain the same since the chamber will be completely insulated with rock wool.

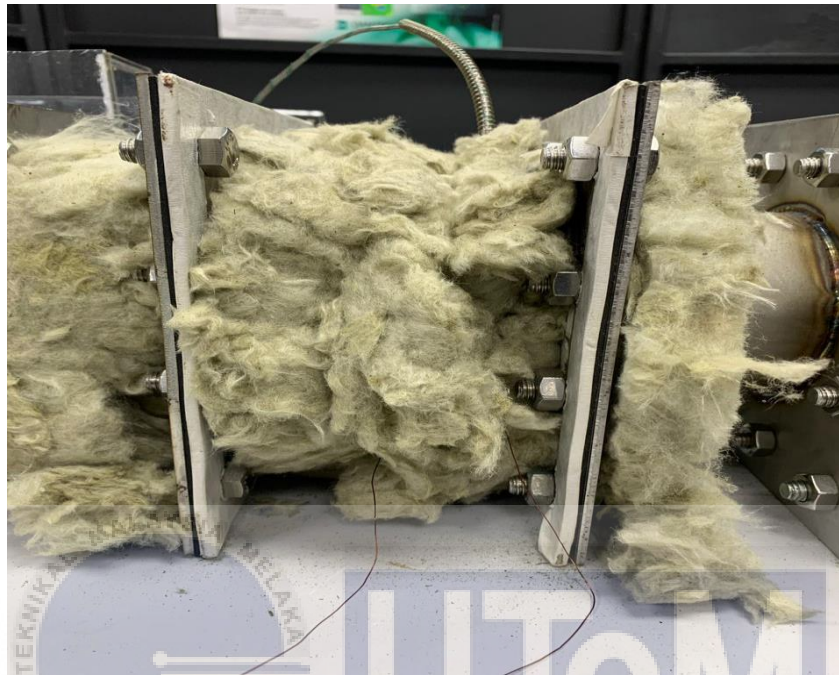


**Figure 3.13 Mineral wool insulation cover**

### **3.6 Limitation of Proposed Methodology**

Due to the fact that the hot chamber size is not big enough, large heating element cannot be used, this is because large heating element needs huge space to be installed. Thus, the heating element size is limited as the chamber inner dimension could not fix large heater. Furthermore, due to the insufficient space inside the chamber, the heating element cannot be installed inside the hot chamber, thus the heating element is placed outside of the chamber which will result in lack of heat distribution.

### 3.7 Summary

This chapter presents the proposed methodology in order to design a hot chamber with heating element as different approach to analyze gas flow in thermal transpiration pump. As the heating element is placed outside of the hot chamber, the temperature of heating element will be controlled by the thermostat. Thus, there will be temperature difference between the heating element and the gas inside the hot chamber. This is because the heat is transferred from the heating element through the object by conduction and the rate of which the heat energy can be transferred can be affected by several factors such as the object's thermal conductivity and the heat transfer coefficients of the fluid or gas surrounding the object. The primary focus of the proposed methodology is to design hot chamber with heating element to heat up the chamber in order to see the temperature difference as well as gas flow.

In general, the gas flow can be analyzed after the hot chamber reached high temperature as the gas inside the chamber drift to the cold end of a narrow channel. This thermal transpiration flow is induced when the boundary walls of the pump have a gradient temperature. Because the pump is based simply on temperature differences and has no moving parts, it could provide reliable and precise control of gas flow for a variety of applications.

## CHAPTER 4

### DISCUSSION

#### 4.1 Introduction

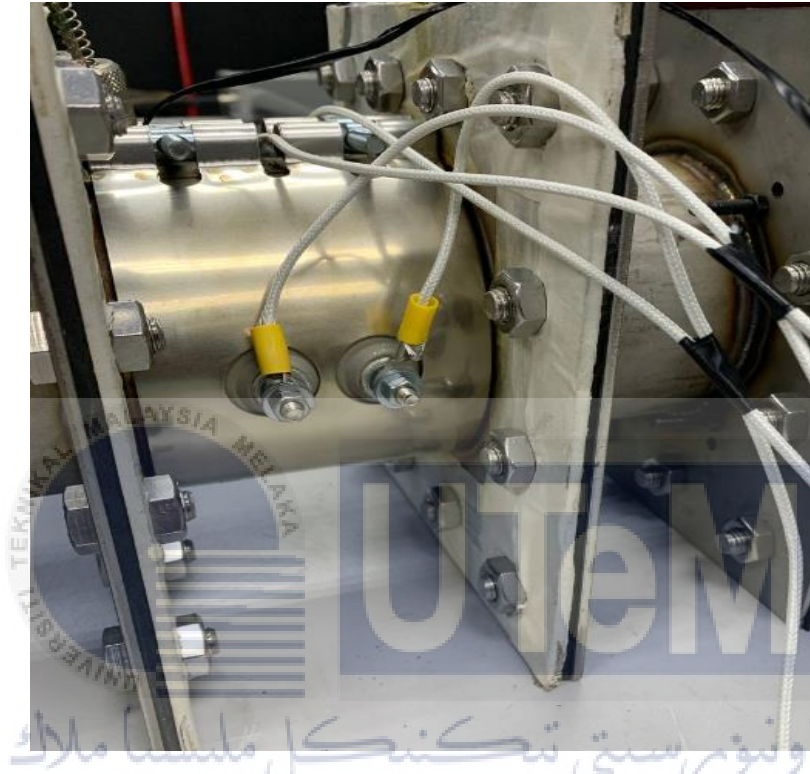
**Table 4-1 Maximum Temperature (°C) vs Time (minutes) parameter**

Maximum Temperature(°C) Parameter	Time (minutes)
150(°C)	15 min

The experiment that is being done to determine the influence of temperature in the hot chamber is being done with three distinct settings, which are the default setting, the setting with insulation (rockwool), and the setting wire mesh with insulation (rockwool). There is no variation in either the temperature or the time parameters for any of these three configurations. The duration of the experiment is 15 minutes, and the highest temperature that may be reached is 150 degrees Celsius. As part of the investigation of the relationship between temperature and time spent in the hot chamber, the results of these tests will be plotted on graph. As the heating element is placed outside the hot chamber surface, this project focus to analyze the temperature inside the hot chamber by placing thermocouple to detect the temperature in °C. The temperature inside the hot chamber and the heating element is different due to several factors. The heating element will heat up the outside surface of the chamber. Thus the temperature inside the hot chamber will not be same as it suffers heat loss via radiation. This is also because the rate at which this heat energy is transferred can

be affected by several factors such as the object's thermal conductivity and the heat transfer coefficients of the gas surrounding the object.

#### 4.2 Initial testing without rockwool and wiremesh



– Figure 4.1 Initial testing without rockwool and wire mesh  
UNIVERSITI TEKNIKAL MALAYSIA MELAKA

#### 4.2.1 Graph Temperature (°C) versus Time (minutes) without cooling system

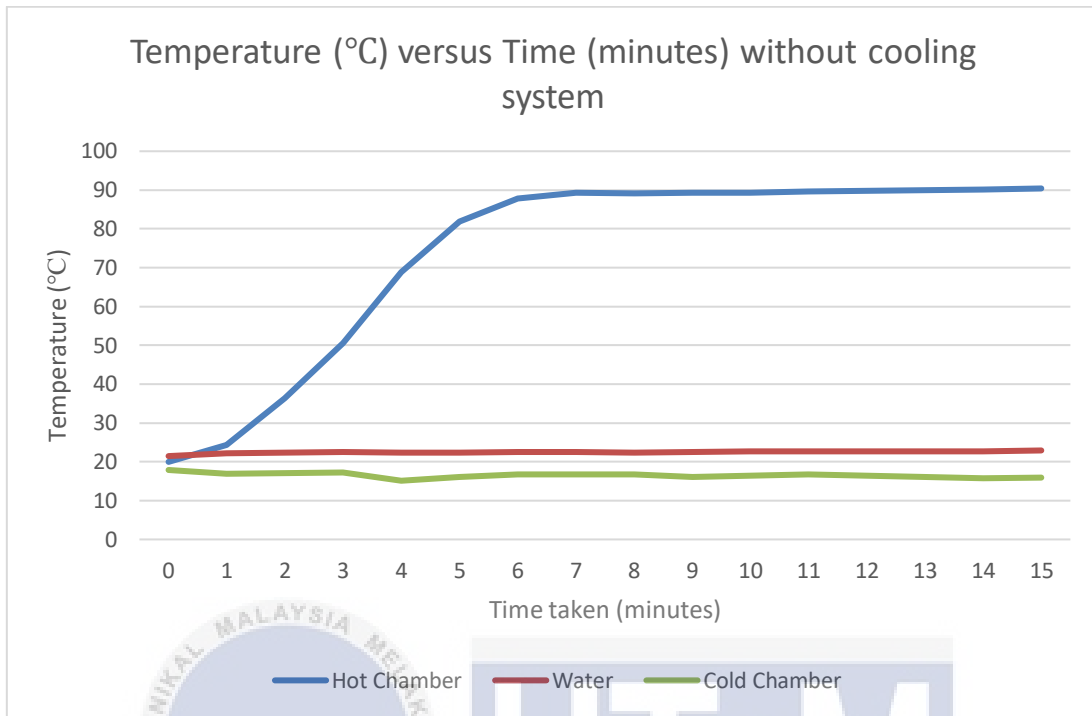


**Figure 4.2 Graph Temperature versus Time without cooling system**

The temperature at the hot chamber (TH1) started to climb exponentially until the 7th minute, at which point the temperature started to maintain and idle. This can be seen from the graph that compares temperature in degrees Celsius to the amount of time in minutes shown above.

This takes place as a result of the fact that after seven minutes, the heat that is supplied by the heater at the hot chamber surface is no longer able to counteract the heat that is lost by the surface of the hot chamber to its surroundings via radiation as it moves along its path. On the other hand, the heat loss due to temperature differences between the heated surface and the environment also affects the temperature inside the hot chamber. Moreover,

the experiment is conducted inside the lab that is air conditioned. Thus, hot chamber suffers heat loss due to its temperature differences.

#### 4.2.2 Graph Temperature (°C) versus Time (minutes) with cooling system

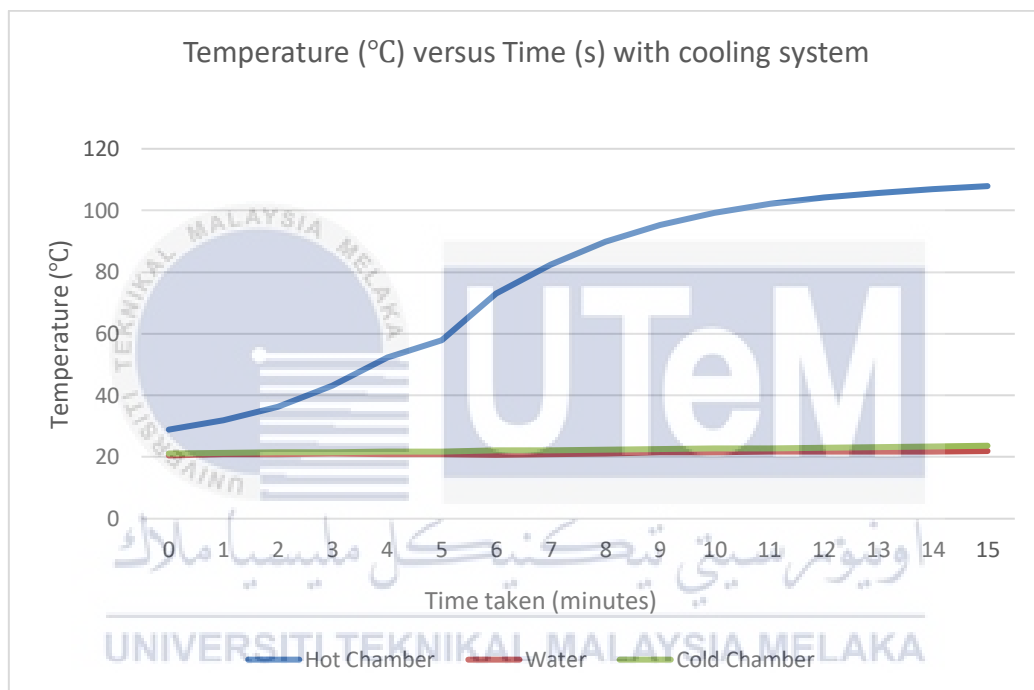


**Figure 4.3 Graph temperature versus time with cooling system**

The initial temperature for this experiment is 28.89°C, as seen in the graph above of temperature (°C) versus time (minutes) with cooling system. The temperature in the hot chamber (TH1) then began to rise, reaching 57.86°C at the end of the fifth minute. This is due to the heater abruptly stopping at the five-minute mark for around ten seconds before restarting to heat the chamber to its maximum temperature of 107.89°C.



According to the graph above, the initial temperature of the experiment was a bit higher than the experiment without a cooling system, which made it easier for the temperature to rise rapidly without experiencing that much of heat loss.

#### 4.2.3 Graph Time versus Temperature Ratio between Tc1 (without cooling system) and Tc2 (with cooling system)

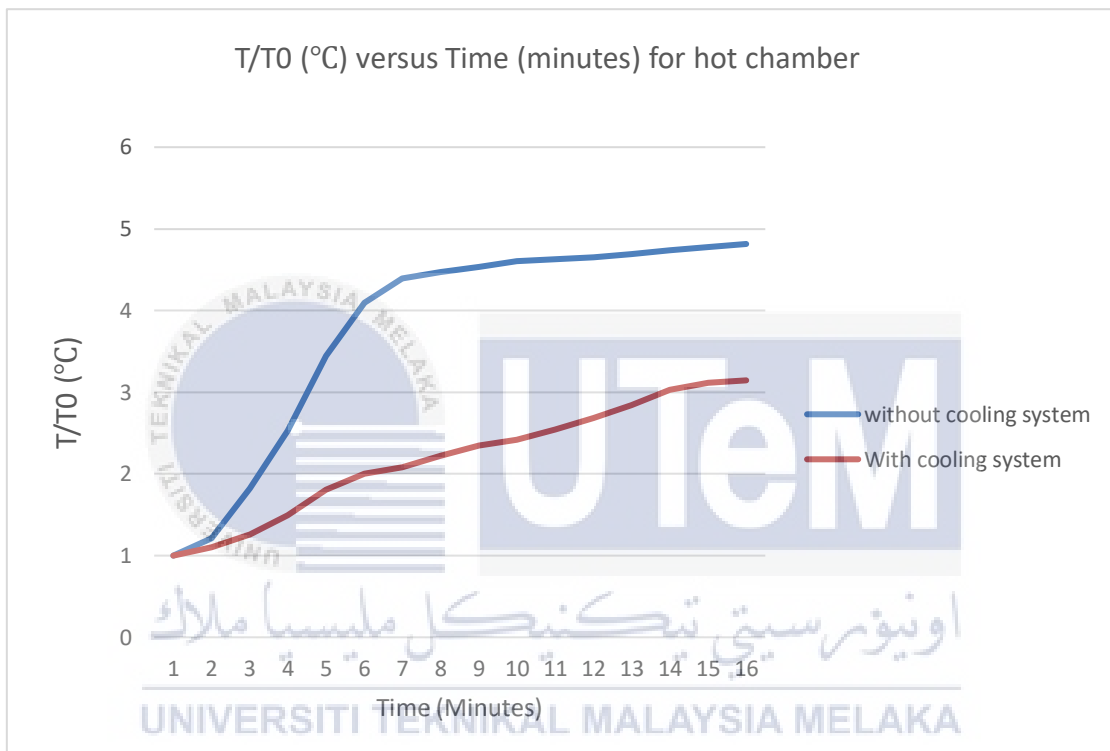


**Figure 4.4 Graph time versus temperature ratio**

The blue line indicates the temperature ratio without a cooling system, while the red line represents the temperature ratio with a cooling system in the graph above showing  $T/T_0$  (°C) versus Time (minutes) for a heated chamber. From the initial data temperature is nearly identical, it is clear from the first data that there is not a significant variation in temperature ratio. However, as the temperature within the chamber continues to rise, it is clear that by minute 6, there is a significant difference in temperature ratio between these two lines. To conclude from the graph that the temperature ratio is larger without a cooling

system than it is with one. This is as a result of how the cooling system affected the rate of temperature.

#### 4.3 Rockwool (with and without cooling system)



Figure 4.5 Rockwool (with and without cooling system)

#### 4.3.1 Graph Temperature (°C) versus Time (minutes) without cooling system

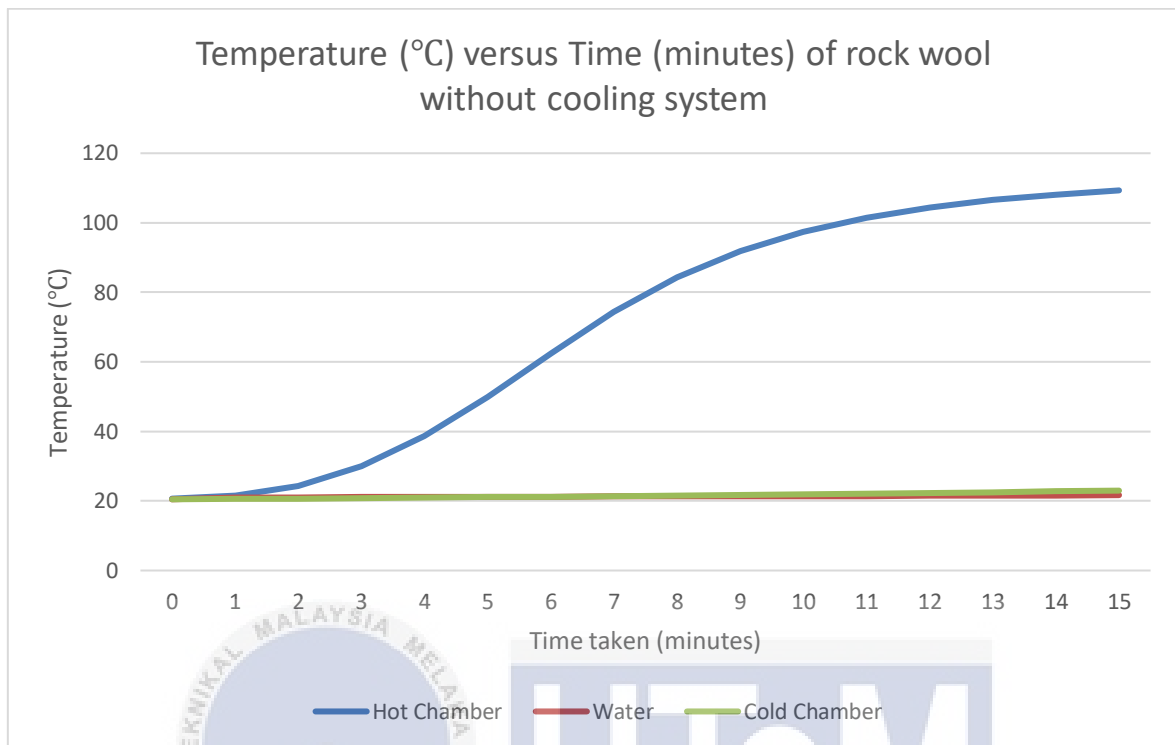


**Figure 4.6 Graph temperature vs time (without cooling system)**

According to the data presented in the temperature (°C) versus time (minutes) graph for rock wool without a cooling system that was shown earlier, the temperature in the hot chamber (TH1) started to grow exponentially after 15 minutes. This was in agreement with the setting that had been specified.

This is the result of the heat being insulated by the rock wool insulation, which in turn allows the temperature to continue to rise without incurring a significant amount of heat loss as a result of radiation.

#### 4.3.2 Graph Temperature (°C) versus Time (minutes) with cooling system

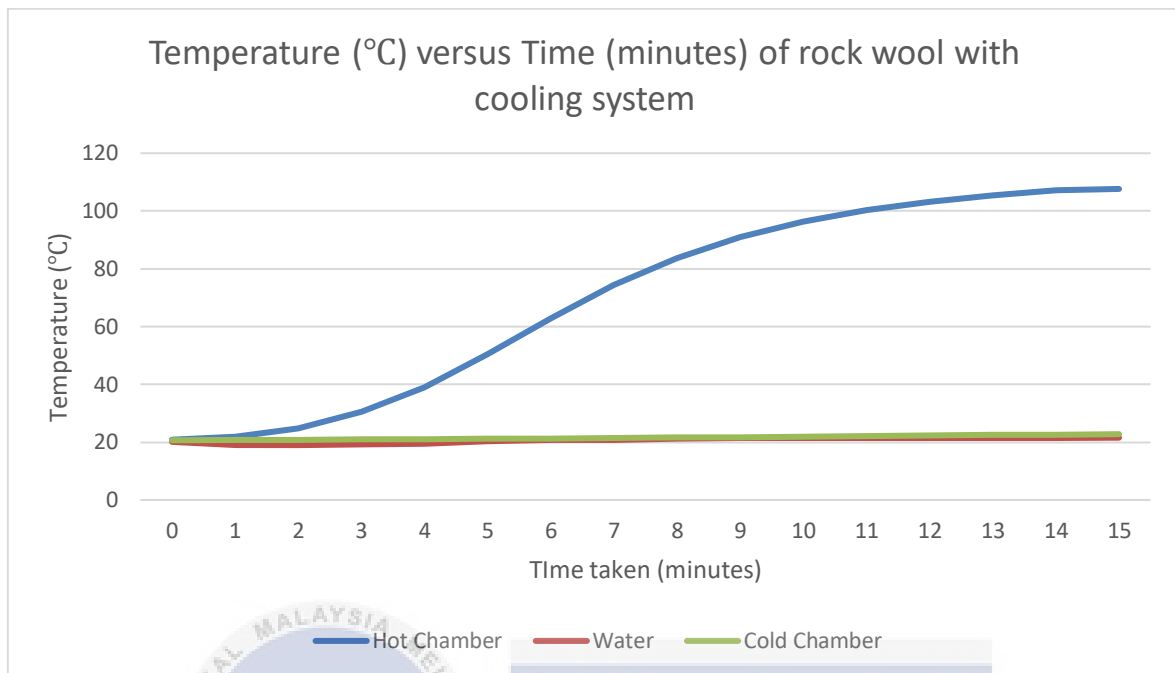


**Figure 4.7 Graph temperature versus time (with cooling system)**

According to the data presented in the graph titled "Temperature (°C) versus Time (minutes) of Rock Wool with Cooling System," which can be found above, the temperature in the hot chamber (TH1) started to rise exponentially after 15 minutes. This was in accordance with the parameter that had been established.

This is the result of the heat being insulated by the rock wool insulation, which in turn allows the temperature to continue to rise without incurring a significant amount of heat loss due to radiation.

### 4.3.3 Graph Comparison Temperature ratio versus Time of rockwool between Tc1 (without cooling system) and Tc2 (with cooling system)

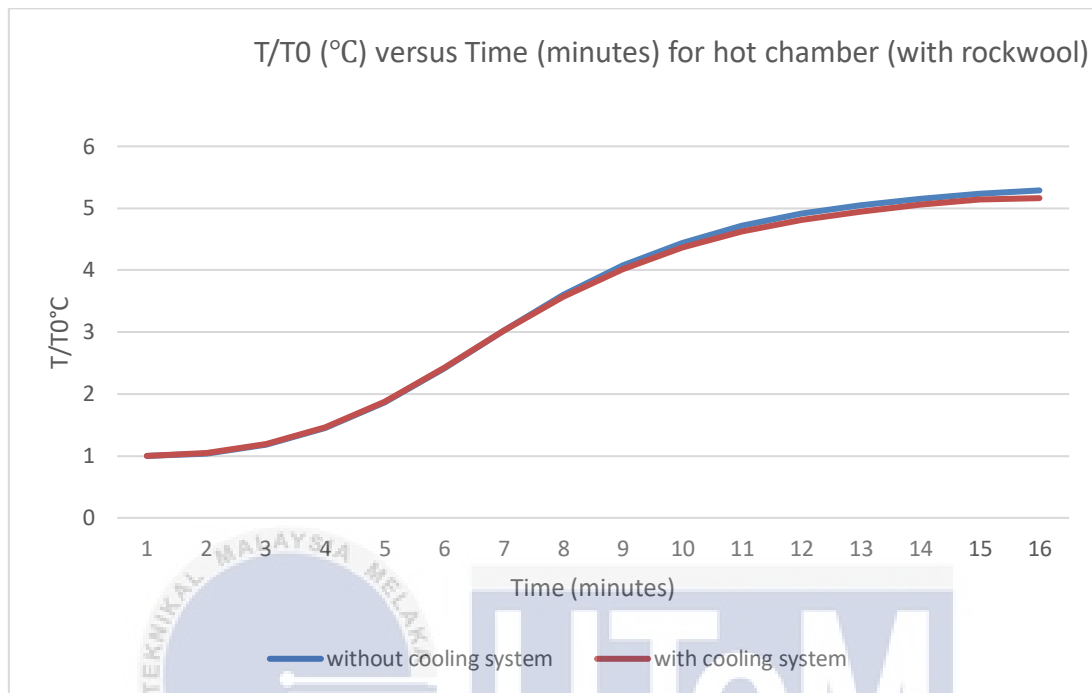


**Figure 4.8 Graph comparison temperature ratio versus time**

The blue line indicates the temperature ratio without a cooling system, while the red line represents the temperature ratio with a cooling system in the graph above showing  $T/T_0$  (°C) vs. Time (minutes) for a heated chamber. We can see from the graph above that there is not much of a change because the insulator (rockwool) plays a crucial function in maintaining the temperature without suffering considerable heat loss. As a result, we may infer from the graph that the temperature ratio is nearly identical because rockwool's ability to insulate heat caused a stable temperature, which in turn decreased heat loss.

#### 4.4 Rockwool + Wiremesh (with and without cooling system)

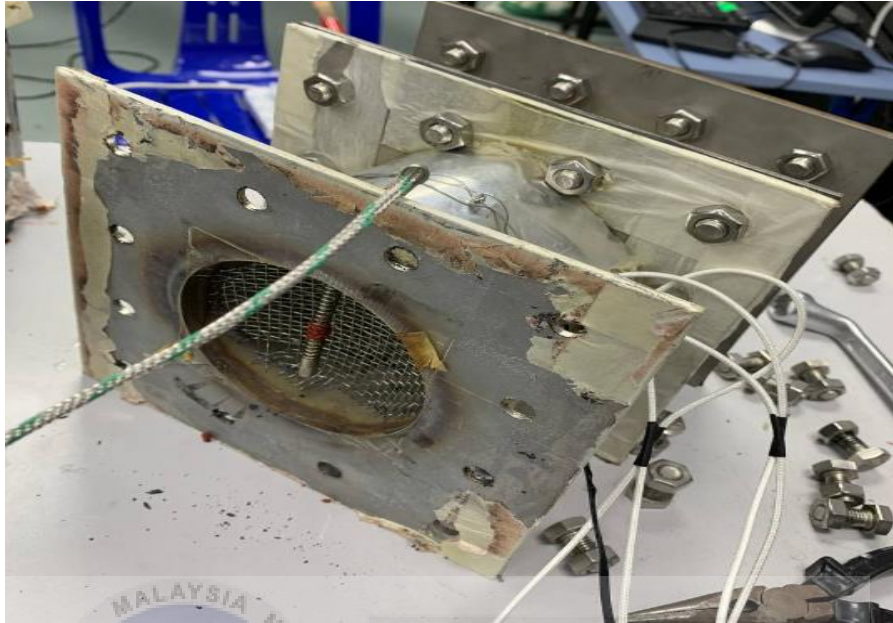
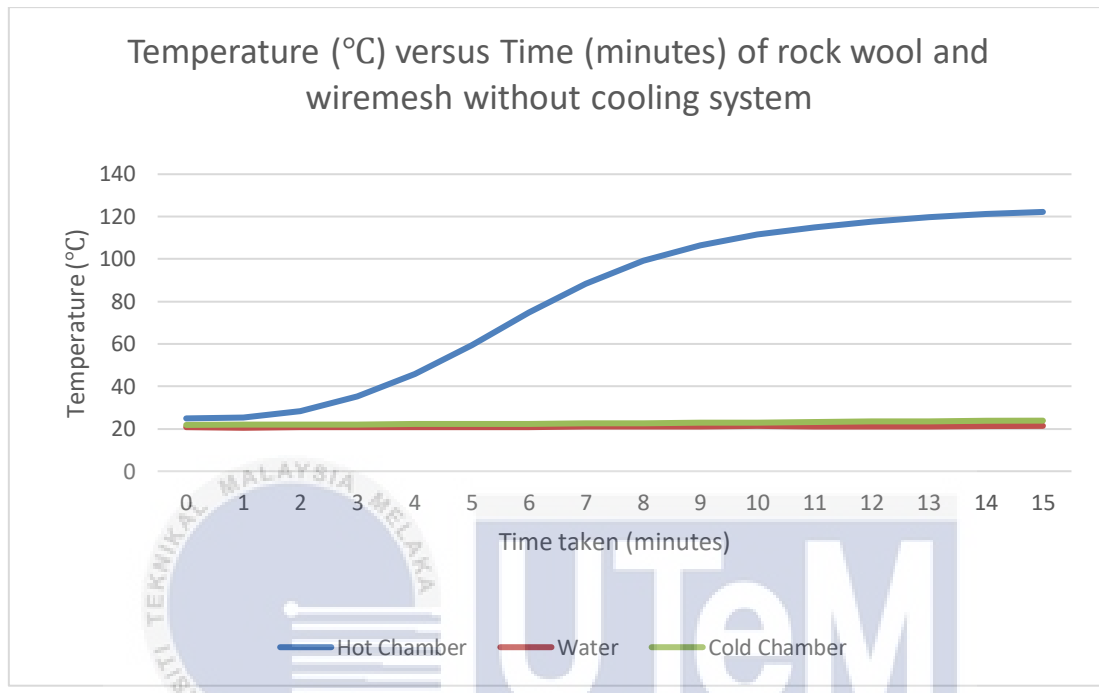


Figure 4.9 Hot chamber with wire mesh and covered by rockwool



#### 4.4.1 Graph temperature versus time of rock wool and wire mesh without cooling system



**Figure 4.10 Graph temperature versus time of rock wool and wire mesh without cooling system**

From the graph temperature (°C) vs Time (minutes) of rock wool + wiremesh without cooling system shown above, temperature at hot chamber (Hot Chamber) started to rise exponentially in accordance with the parameter that has been set which was 15 minutes.

This occurs because rock wool insulation proved that the heat is insulated which then allow the temperature to keep on rising without experiencing that much of heat loss via radiation. On the other hand, wire mesh that has been placed inside the hot chamber plays a big role in the heat distribution via conduction.

#### 4.4.2 Graph temperature versus time of rock wool and wire mesh with cooling system

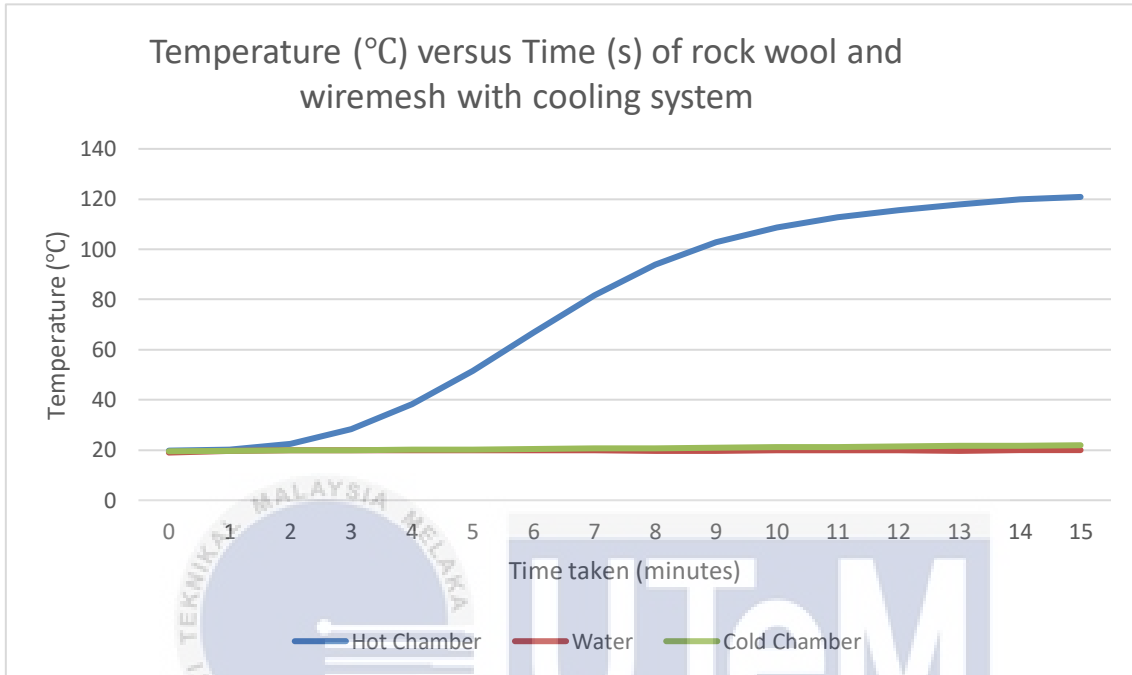


**Figure 4.11 Graph Temperature (°C) versus Time (minutes) with cooling system**

The temperature in the heated chamber (Hot Chamber) began to climb exponentially in accordance with the parameter that had been set, which was 15 minutes, as can be seen in the graph that compares temperature in degrees Celsius to time in minutes that was given above.

This is the result of the heat being insulated by the rock wool insulation, which in turn allows the temperature to continue to rise without incurring a significant amount of heat loss as a result of radiation. Wiremesh, on the other hand, which has been installed inside the hot chamber, plays a significant part in the conduction of heat.



**4.4.3 Graph comparison temperature ratio vs time of rockwool + wire mesh between hot chamber without cooling system and hot chamber with cooling system.**

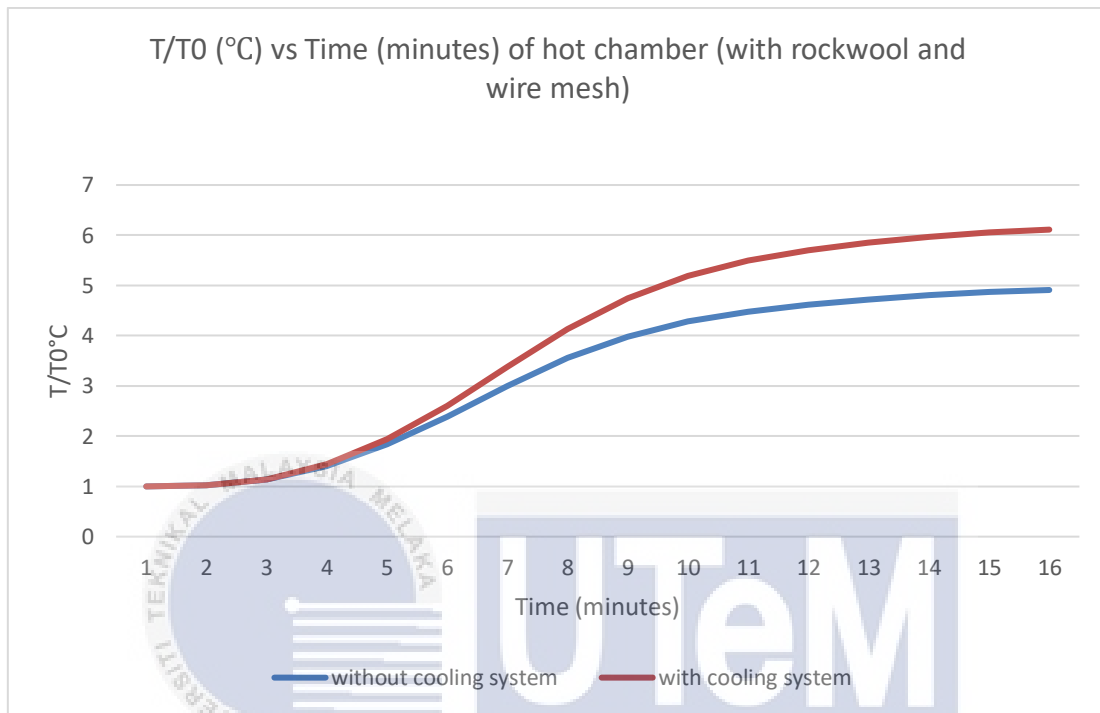


**Figure 4.12 Graph temperature ratio versus time**

The blue line indicates the temperature ratio without a cooling system, while the red line represents the temperature ratio with a cooling system in the graph above showing  $T/T_0$  (°C) vs. Time (minutes) for a heated chamber. Initially there is not much of a change because the insulator (rockwool) and wire mesh (heat distributor) play crucial functions in maintaining the temperature as well as giving great temperature distribution inside the hot chamber without suffering that much amount of heat loss. However, on minute 6, the difference started to be seen as the red line (without cooling system) started to rise higher.

**4.5 Comparison of maximum temperature between hot chamber (Th), cold chamber (Tc), water (Tw) with and without cooling system.**

**Table 4-2 Comparison of maximum temperature between (Th), (Tc), and (Tw) with cooling system**

Parameter	Th(°C)	Tc(°C)	Tw(°C)
Initial	90.87°C	23.67°C	21.94°C
Rockwool	107.65°C	22.76°C	21.55°C
Rockwool + Wire mesh	120.84°C	23.84°C	21.23°C

From the table above, the temperature of hot chamber (Th) for initial is 90.87°C, the temperature of hot chamber (Th) using insulator (rockwool) is 107.65°C, and the temperature of hot chamber (Th) using insulator (rockwool) and wire mesh is 120.84°C. From the results of the experiment, there is significant increase of temperature from initial, rockwool, and rockwool + wire mesh. This is because the rockwool able to reduce significant heat loss via radiation. In addition, the wire mesh able to provide heat distribution from the hot chamber surface to pass through inside the hot chamber. From the table above, there is not that much difference for Tc and Tw as the cooling system functions well to reduce the heat that influenced hot chamber to cold chamber.

**Table 4-3 Comparison of maximum temperature between (Th), (Tc), and (Tw) without cooling system**

Parameter	Th(°C)	Tc(°C)	Tw(°C)
Initial	90.41°C	15.91°C	22.92°C
Rockwool	109.31°C	22.97°C	21.68°C
Rockwool + Wire mesh	122.22°C	21.23°C	23.83°C

From the table above, the temperature of hot chamber (Th) for initial is 90.41°C, the temperature of hot chamber (Th) using insulator (rockwool) is 109.31°C, and the temperature of hot chamber (Th) using insulator (rockwool) and wire mesh is 122.22°C. From the results of the experiment, there is significant increase of temperature from initial, rockwool, and rockwool + wire mesh. This is because the rockwool able to reduce significant heat loss via radiation. In addition, the maximum temperature of hot chamber (Th) for these three experiments (initial, rockwool, rockwool + wire mesh) are higher compared to experiments with cooling system. This is because the cooling system affects the heating which will also affect the maximum temperature. From the table above, there is not that much difference for Tc and Tw as the cooling system functions well to reduce the heat that influenced hot chamber to cold chamber.

#### 4.6 Heat Distribution on Thermal Camera

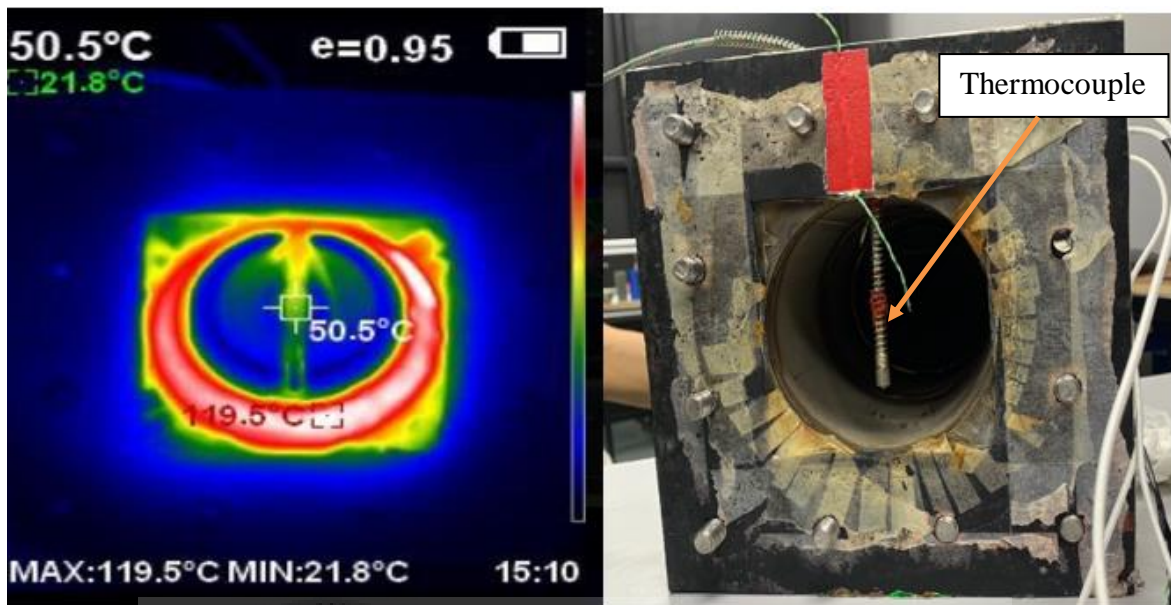


**Figure 4.13 Heat distribution on thermal camera for empty hot chamber**

Brighter colours (red, orange, and yellow) imply higher temperatures (more heat and infrared radiation being released), but darker colours (purples and dark blue/black hues) indicate lower temperatures (less heat and infrared radiation emitted). The aluminium surface that is heated by the heating element is shown in the figure above with a red region, which shows that this is the area that is the hottest. From the figure above, hot chamber surface is 119.5(°C) while the temperature inside the chamber which is blue colour is 50.5(°C). From both temperature difference, due to heat loss through radiation, the rate of heat distribution is slow to reach inside the hot chamber from the two temperature differences.

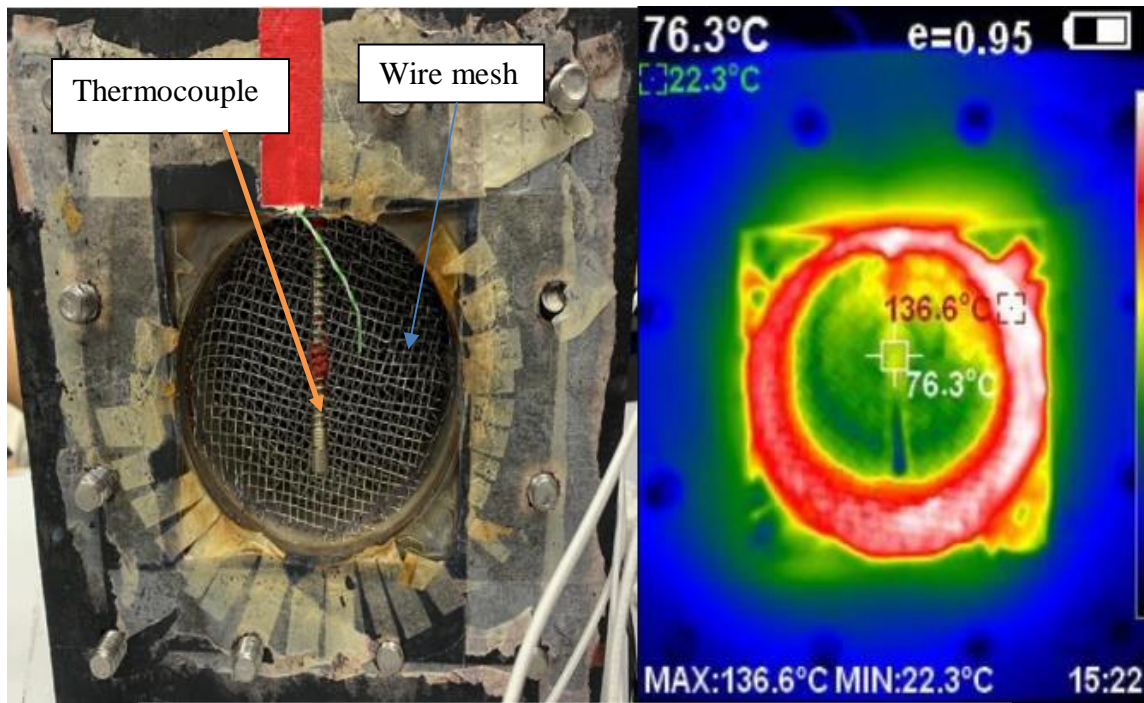


**Figure 4.14 Heat distribution on thermal camera for installed wire mesh chamber**

Brighter colours (red, orange, and yellow) imply higher temperatures (more heat and infrared radiation being released), but darker colours (purples and dark blue/black hues) indicate lower temperatures (less heat and infrared radiation emitted). The aluminium surface that is heated by the heating element is shown in the figure above with a red region, which shows that this is the area that is the hottest. The presence of a yellow colour inside the hot chamber indicates that heat is being conducted from a heated region (shown by red) to a cooler region (represented by green) via conduction. Because of the use of the wire mesh that is placed inside the hot chamber, there is proper distribution of heat within the hot chamber itself. Moreover, the thermal conductivity of the wire mesh allows the heat to transfer and distributed well inside the chamber as it transfers heat more rapidly.

## CHAPTER 5

### CONCLUSION AND RECOMENDATION

#### 5.1 Conclusion

The main focus of this project is to review and identify the parameters that effect the performance of thermal transpiration pump, to evaluate the effect of hot chamber parameters on the temperature, and to analyse the effect of temperature difference on the gas flow properties in the thermal transpiration pump. From the results that have been obtained from the experiments, the temperature gradient without using cooling system is higher compared to with cooling system as the cooling system will limit the higher temperature that can be heated by the hot chamber.

Multiple experiments have shown that utilising rockwool as an insulator and wire mesh as a heat distributor allows the inside temperature of the hot chamber to raise to much higher temperatures than it could without them. The reason for this is the significant heat loss. Radiational heat loss occurs as heat from the heating element travels from the surface of the hot chamber into the interior of the hot chamber. As a result, the maximum temperature achieved is significantly lower than when an insulator and wire mesh were used.

Last but not least, as the temperature rises until its maximum. the temperature at hot chamber will influence the temperature at cold chamber, this can be seen as the temperature reaches its maximum, the temperature of cold chamber also increases as the flow is

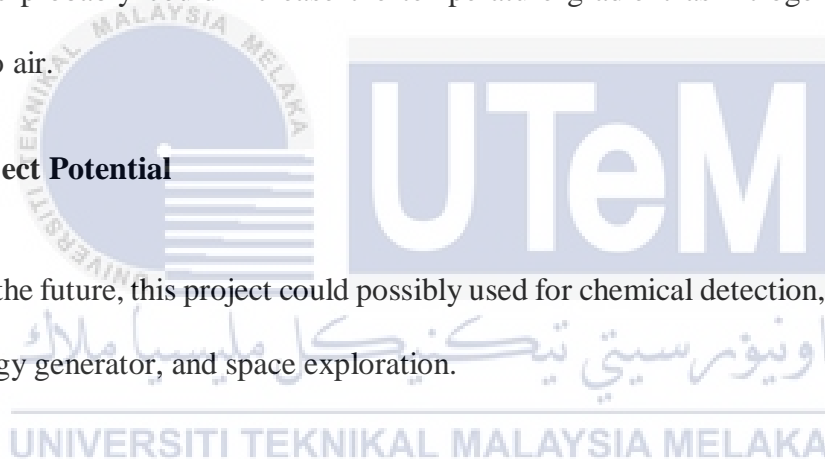
happening through the porous media channel. In summary, the goals of this experiment were successfully accomplished, making it a successful experiment overall.

## 5.2 Recommendation

If the heating element were to undergo certain modifications, this project might become more functional. This is because there is a greater potential for the transfer of heat within the chamber, which will lead to an increase in the temperature gradient. On the other side, the insulator might also be upgraded to reduce the amount of heat that is lost as a result of radiation as it is travelling to the chamber from its starting point. In addition, using nitrogen gas probably could increase the temperature gradient as nitrogen gas is lighter compared to air.

## 5.3 Project Potential

In the future, this project could possibly used for chemical detection, environmental health, energy generator, and space exploration.



## REFERENCES

- Nagy, B., Simon, T. K., & Nemes, R. (2020). Effect of built-in mineral wool insulations durability on its thermal and mechanical performance. *Journal of Thermal Analysis and Calorimetry*, 139(1), 169–181. <https://doi.org/10.1007/s10973-019-08384-5>.
- Gao, S., Sun, R., Feng, Y., & Hao, J. (2021). Research Progress of Wearable Electric Heating Elements. *Thermal Science*, 25(3), 2289–2293. <https://doi.org/10.2298/TSCI200601117G>.
- Ngo, T. T., Zhou, T., Nguyen, H. Van, Nguyen, P. M., & Lee, G. S. (2021). New design of a hot mixing chamber for lowering its surface temperature by adopting a perforated inner cylinder. *Journal of Mechanical Science and Technology*, 35(12). <https://doi.org/10.1007/s12206-021-1141-8>.
- Rattanakaran, J., Saengrayap, R., Aunsri, N., Padee, S., Prahsarn, C., Kitazawa, H., ... Chaiwong, S. (2021). Performance of thermal insulation covering materials to reduce postharvest losses in okra. *Horticulturae*, 7(10). <https://doi.org/10.3390/horticulturae7100392>.
- Fang, S., Wang, R., Ni, H., Liu, H., & Liu, L. (2020). A review of flexible electric heating element and electric heating garments. *Journal of Industrial Textiles*, (399), 1–36. <https://doi.org/10.1177/1528083720968278>.
- Hajatzadeh Pordanjani, A., Aghakhani, S., Afrand, M., Mahmoudi, B., Mahian, O., & Wongwises, S. (2019). An updated review on application of nanofluids in heat exchangers



for saving energy. *Energy Conversion and Management*, 198(April), 111886.  
<https://doi.org/10.1016/j.enconman.2019.111886>.

Ž, C. Š., Āžā, Š. Ž., & Si, Ö. (1950). on Molybdenum Disilicide By Heating Elements Shigetomo ( Central Tomitaro Tokyo Shibaura KUBO \* Electric Kazumoto HOMMA \*\* Denko Co ., Ltd .) Co ., Ltd ., \*\* Toshiba at MO3Si, 2.

Zhang, Z., Wang, X., Zhao, L., Zhang, S., & Zhao, F. (2019). Study of flow characteristics of gas mixtures in a rectangular Knudsen pump. *Micromachines*, 10(2).  
<https://doi.org/10.3390/mi10020079>.

N'ein, Z. N., Serikov, A. V., & Serikov, V. A. (2019). Analysis of the Thermal State of a Heating Element of Transformer Type. *Russian Electrical Engineering*, 90(5), 397–401.  
<https://doi.org/10.3103/S1068371219050110>.

Gupta, N. K., & Gianchandani, Y. B. (2010). A high-flow Knudsen pump using a polymer membrane: Performance at and below atmospheric pressures. *Proceedings of the IEEE International Conference on Micro Electro Mechanical Systems (MEMS)*, 1095–1098.  
<https://doi.org/10.1109/MEMSYS.2010.5442401>

Abdullah, R., and Rodzi, A.M., 2011. Labor Utilization and Man to Machine Ratio Study at a Semiconductor Facility. *Journal of Engineering and Technology (JET)*, 2, pp. 75-84.

Rahman, M.N., Abdullah, R., and Kamarudin, N., 2012. Work Study Techniques Evaluation At Back-End Semiconductor Manufacturing. *Proceedings of the 2012 International Conference on Design and Concurrent Engineering*, Melaka, Malaysia, 2, pp. 24-27.

Sone, Y. (2003). *Vacuum Pump without a Moving Part and its Performance*.

<https://doi.org/10.1063/1.1581654>



## APPENDIX

PSM1															
No.	Activity	WEEK													
		1	2	3	4	5	6	7	8	9	10	11	12	13	14
1	Purchasing Components for Hot Chamber														
2	Installation of Hot Chamber														
3	Installation of Heating Element														
4	Run Experiment, Data Collection, and Thesis Writing														
5	Correction of PSM 2 Report														
6	Presentation														

7	Submission of Final PSM 2 Report																	
---	-------------------------------------	--	--	--	--	--	--	--	--	--	--	--	--	--	--	--	--	--

**APPENDIX 1 Gantt chart PSM 2**

Data Default testing without rockwool and wire mesh

temperature hot chamber				
Time taken (minutes)	T <sub>H1</sub>	T <sub>H2</sub>	without cc	with cooling system
0	19.98	28.89	1	1
1	24.28	31.93	1.215215	1.105227
2	36.36	36.38	1.81982	1.259259
3	50.55	43.09	2.53003	1.49152
4	68.89	52.2	3.447948	1.806854
5	81.84	57.86	4.096096	2.002769
6	87.77	60.11	4.392893	2.080651
7	89.33	64.11	4.470971	2.219107
8	89.17	67.89	4.532963	2.349948
9	89.28	69.9	4.608468	2.419522
10	90.21	73.41	4.631502	2.541018
11	90.56	77.65	4.652533	2.687781
12	90.78	82.09	4.693544	2.841468
13	90.79	87.53	4.734044	3.029768
14	90.89	89.98	4.779049	3.114573
15	90.91	90.87	4.815055	3.145379

**APPENDIX 2 Data default testing without rockwool and wire mesh**

Data Rockwool (with and without cooling system)

temperature hot chamber				
Time taken (minutes)	T <sub>H1</sub>	T <sub>H2</sub>	without cooling system	with cooling system
0	20.67	20.85	1	1
1	21.47	21.82	1.038703	1.046523
2	24.38	24.78	1.179487	1.188489
3	30.07	30.46	1.454765	1.460911
4	38.61	39	1.867925	1.870504
5	49.81	50.41	2.409773	2.417746
6	62.47	62.94	3.022254	3.018705
7	74.35	74.41	3.597	3.568825
8	84.23	83.77	4.074988	4.017746
9	91.85	90.99	4.443638	4.364029
10	97.43	96.37	4.713595	4.622062
11	101.49	100.24	4.910015	4.807674
12	104.43	103.15	5.05225	4.947242
13	106.58	105.46	5.156265	5.058034
14	108.15	107.17	5.232221	5.140048
15	109.31	107.65	5.288341	5.16307

UNIVERSITI TEKNIKAL MALAYSIA MELAKA  
**APPENDIX 3 Data rockwool (with and without cooling system)**

Rockwool + wire mesh (with and without cooling system)

**Table 5-1 Rockwool + wire mesh (with and cooling system)**

temperature hot chamber				
Time taken (minutes)	$T_{H1}$	$T_{H2}$	without cc	with cooling system
0	24.89	19.77	1	1
1	25.41	20.15	1.020892	1.019221
2	28.38	22.5	1.140217	1.138088
3	35.13	28.43	1.41141	1.438037
4	45.75	38.25	1.838088	1.93475
5	59.47	51.44	2.389313	2.601922
6	74.64	66.75	2.998795	3.376328
7	88.49	81.7	3.555243	4.132524
8	99.14	93.92	3.983126	4.750632
9	106.52	102.68	4.27963	5.193728
10	111.46	108.6	4.478104	5.493171
11	114.91	112.66	4.616714	5.698533
12	117.52	115.62	4.721575	5.848255
13	119.6	117.94	4.805143	5.965604
14	121.31	119.82	4.873845	6.060698
15	122.22	120.84	4.910406	6.112291

## FAKULTI TEKNOLOGI KEJURUTERAAN MEKANIKAL DAN PEMBUATAN

Tel : +606 270 1184 | Faks : +606 270 1064

Rujukan Kami (Our Ref):  
Rujukan Tuan (Your Ref):  
Tarikh (Date): 31 Januari 2021

Chief Information Officer  
Perpustakaan Laman Hikmah  
Universiti Teknikal Malaysia Melaka

Melalui

Dekan  
Fakulti Teknologi Kejuruteraan Mekanikal dan Pembuatan  
Universiti Teknikal Malaysia Melaka

Tuan

### PENKELASAN TESIS SEBAGAI TERHAD BAGI TESIS PROJEK SARJANA MUDA

Dengan segala hormatnya merujuk kepada perkara di atas.

2. Dengan ini, dimaklumkan permohonan pengkelasan tesis yang dilampirkan sebagai TERHAD untuk tempoh **LIMA** tahun dari tarikh surat ini. Butiran lanjut laporan PSM tersebut adalah seperti berikut:

**Nama pelajar: ILMAN HAKIM BIN MUHAMAD JAMALUDIN**

**Tajuk Tesis: EFFECT OF HOT CHAMBER PARAMETER ON THE GHAS FLOW IN THE THERMAL TRANSPIRATION PUMP.**

3. Hal ini adalah kerana IANYA MERUPAKAN PROJEK YANG DITAJA OLEH SYARIKAT LUAR DAN HASIL KAJIANNYA ADALAH SULIT.

Sekian, terima kasih.

**“BERKHIDMAT UNTUK NEGARA”**  
**“KOMPETENSI TERAS KEGEMILANGAN”**

Saya yang menjalankan amanah,

**PN. SUSHELLA EDAYU BINTI MAT KAMAL**

Penyelia Utama/ Pensyarah Kanan  
Fakulti Teknologi Kejuruteraan Mekanikal dan Pembuatan  
Universiti Teknikal Malaysia Melaka